Check for updates

Received: 2 March 2021 | Revised: 29 September 2021 | Accepted: 30 September 2021

DOI: 10.1111/gcb.15951

PRIMARY RESEARCH ARTICLE

Global Change Biology WILEY

Living, dead, and absent trees—How do moth outbreaks shape small-scale patterns of soil organic matter stocks and dynamics at the Subarctic mountain birch treeline?

Nele Meyer[1,2] | Yi Xu[1] | Katri Karjalainen[3] | Sylwia Adamczyk[1,4] | Christina Biasi[3] | Lona van Delden[3,5] | Angela Martin[1] | Kevin Mganga[1,6] | Kristiina Myller[3] | Outi-Maaria Sietiö[1] | Otso Suominen[7] | Kristiina Karhu[1,8]

[1]Department of Forest Sciences, Faculty of Agriculture and Forestry, University of Helsinki, Helsinki, Finland

[2]Department of Soil Ecology, University of Bayreuth, Bayreuth, Germany

[3]Department of Environmental and Biological Sciences, University of Eastern Finland, Kuopio, Finland

[4]Natural Resources Institute Finland (Luke), Helsinki, Finland

[5]Alfred Wegener Institute Helmholtz Centre for Polar and Marine Research, Potsdam, Germany

[6]Department of Agricultural Sciences, South Eastern Kenya University, Kitui, Kenya

[7]Biodiversity Unit, Kevo Subarctic Research Institute, University of Turku, Turku, Finland

[8]Helsinki Institute of Life Science (Hilife), University of Helsinki, Helsinki, Finland

Correspondence
Nele Meyer, Department of Forest Sciences, Faculty of Agriculture and Forestry, University of Helsinki, Helsinki, Finland.
Email: nele.meyer@uni-bayreuth.de

Funding information
Suomen Akatemia, Grant/Award Number: 316401

Abstract

Mountain birch forests (*Betula pubescens* Ehrh. ssp. *czerepanovii*) at the subarctic treeline not only benefit from global warming, but are also increasingly affected by caterpillar outbreaks from foliage-feeding geometrid moths. Both of these factors have unknown consequences on soil organic carbon (SOC) stocks and biogeochemical cycles. We measured SOC stocks down to the bedrock under living trees and under two stages of dead trees (12 and 55 years since moth outbreak) and treeless tundra in northern Finland. We also measured in-situ soil respiration, potential SOC decomposability, biological (enzyme activities and microbial biomass), and chemical (N, mineral N, and pH) soil properties. SOC stocks were significantly higher under living trees (4.1 ± 2.1 kg m^2) than in the treeless tundra (2.4 ± 0.6 kg m^2), and remained at an elevated level even 12 (3.7 ± 1.7 kg m^2) and 55 years (4.9 ± 3.0 kg m^2) after tree death. Effects of tree status on SOC stocks decreased with increasing distance from the tree and with increasing depth, that is, a significant effect of tree status was found in the organic layer, but not in mineral soil. Soil under living trees was characterized by higher mineral N contents, microbial biomass, microbial activity, and soil respiration compared with the treeless tundra; soils under dead trees were intermediate between these two. The results suggest accelerated organic matter turnover under living trees but a positive net effect on SOC stocks. Slowed organic matter turnover and continuous supply of deadwood may explain why SOC stocks remained elevated under dead trees, despite the heavy decrease in aboveground C stocks. We conclude that the increased occurrence of moth damage with climate change would have minor effects on SOC stocks, but ultimately decrease ecosystem C stocks (49% within 55 years in this area), if the mountain birch forests will not be able to recover from the outbreaks.

KEYWORDS
deadwood, insect herbivory, microbial N mining, priming effect, Soil organic carbon, soil respiration

This is an open access article under the terms of the Creative Commons Attribution License, which permits use, distribution and reproduction in any medium, provided the original work is properly cited.
© 2021 The Authors. *Global Change Biology* published by John Wiley & Sons Ltd.

1 | INTRODUCTION

Mountain birch (*Betula pubescens* Ehrh. ssp. *czerepanovii*) is the dominant tree species at the subarctic treeline of Fennoscandia, and significantly contributes to the CO_2 sink capacity of subarctic landscapes (Christensen et al., 2007). Due to climate warming and increased nitrogen (N) deposition, an advance of the treeline has been observed in recent decades (Hofgaard et al., 2012; Rundqvist et al., 2011; Tømmervik et al., 2004). Global warming has also led to a drastic increase in insect herbivory over the past decades (Hagen et al., 2007; Jepsen et al., 2007; Neuvonen et al., 1999). Insect herbivory has been shown to have immense impacts on plant growth and carbon (C) fluxes, even at background intensities (Silfver et al., 2020), but outbreak intensities in particular cause large natural disturbances. For instance, Heliasz et al. (2011) reported an 89% reduction of the C sink strength upon defoliation of mountain birch by larvae of autumn and winter moths. In Fennoscandia, outbreaks of caterpillars from foliage-feeding geometrid moths (*Epirrita autumnata* and *Operophtera brumata*) occur at intervals of around 10 years. While mountain birch can compensate defoliation to some extent (Huttunen et al., 2012), intense damage in such nutrient-poor soils and in cold climatic conditions often leads to forest dieback, leaving large areas of deadwood behind (Tenow, 1996). Considering that 5,000 km^2 of mountain birch forest were affected in the 1960s in northern Finland alone (Nuorteva, 1963), and 10,600 km^2 during the 2000s in northern Fennoscandia (Jepsen et al., 2009), this issue is of quantitative relevance. High intensity summer grazing by reindeer compounds the issue by impeding the growth of new birch seedlings and basal sprouts, especially in Finnish Lapland (Biuw et al., 2014; Kumpula et al., 2011; Lehtonen & Heikkinen, 1995). The combination of grazing and moth damage induces a conversion of former forests into treeless tundra vegetation, resulting in immense reductions of tree primary production (Olsson et al., 2017), and thus, CO_2 sequestration potential.

The consequences of treeline advance or forest dieback on aboveground C storage are straightforward and frequently studied (Dahl et al., 2017; Russell et al., 2015); however, the consequences on soil organic carbon (SOC) stocks are rather uncertain. Several studies have shown that an advance of the treeline may deplete SOC stocks (Clemmensen et al., 2021; Friggens et al., 2020; Hartley et al., 2012; Wilmking et al., 2006) despite C input via litter and roots. For instance, Parker et al. (2015) showed that SOC stocks of organic layers were considerably lower in forested plots (2.04 ± 0.25 kg m^2) than at heath plots (7.03 ± 0.79 kg m^2). This may be explained by a phenomenon termed the "priming effect" (Fontaine et al., 2004; Kuzyakov et al., 2000): a labile C supply from root exudates or fresh litter can stimulate microbial decomposition of older soil organic matter (SOM). In this context, it is assumed that microbes increasingly decompose SOM to acquire N from it ("microbial N-mining"; Craine et al., 2007; Moorhead & Sinsabaugh, 2006), which is particularly relevant in N-poor subarctic soils (Hicks et al., 2020).

Reversing this finding, it may be speculated that despite the decrease in tree primary production, forest dieback caused by moth outbreaks can induce an increase of SOC stocks, for at least five reasons. First, root exudation decreases, which then causes a decrease in labile C that can stimulate priming. Second, insect herbivory induces an abrupt return of available N and other nutrients to soils via frass (Kaukonen et al., 2013; Parker et al., 2017). Together with the lower N demand of dead trees, the limits on N may be released, hence N-mining and associated priming become unnecessary in soil that is no longer N-limited. Third, large amounts of organic matter are returned to the soil via decomposing roots and deadwood (Kosunen et al., 2020). Since SOM decomposes slowly in cold climates, and parts of SOM are recalcitrant or stabilized and can remain in soil for hundreds or thousands of years (Lehmann & Kleber, 2015; Schmidt et al., 2011), elevated SOC stocks may persist in the long term. Fourth, temporal patterns of deadwood decay usually follow a negative exponential curve (Mackensen & Bauhus, 2003), that is, SOM turnover rates may slow down once the most labile compounds of decaying wood have been mineralized. Fifth, insect herbivory has been found to change vegetation composition from shrub-dominated to grass-dominated plant communities (Karlsen et al., 2013), possibly associated with larger organic matter input into soil. Indeed, reduced soil CO_2 efflux has been observed immediately after a defoliation event (Parker et al., 2017) and 8 years thereafter (Sandén et al., 2020), suggesting slowed biochemical cycling. However, despite decreased turnover rates, Sandén et al. (2020) found no difference in SOC stocks 8 years after a defoliation event of subarctic mountain birch in northern Fennoscandia.

Interestingly, the opposite effect (i.e., higher resource turnover rates in the short term) have been observed after moth outbreaks (Kaukonen et al., 2013; Kristensen et al., 2018), mainly linked to increasing concentrations of soil mineral N and labile C from moth frass. According to Kaukonen et al. (2013), moth outbreaks represent a shortcut in C and N input to soils, which bypasses the main routes of carbon from plants to the soil via mycorrhizal and litter-decomposing fungi. However, it remains uncertain whether this effect persists in the long term. From a study on coniferous forests, Štursová et al. (2014) speculated that the rate of decomposition decreases as soon as the one-time litter input had been processed. Similarly, Kristensen et al. (2018) assumed that such increased turnover rates are mainly short-lived effects, while lower turnover rates can be expected in the long term. Overall, the temporal effects of moth outbreaks and associated tree death on SOM stocks and biochemical cycling are poorly understood. In particular, the long-term effects are not well quantified.

Former studies on the effect of treeline advance or retreat suffer from the drawback that forested sites are compared with separate tundra sites, or forested sites with defoliated sites, respectively (Hartley et al., 2012; Wilmking et al., 2006). Such space-for-time substitutions are prone to confounding effects, such as differences in temperature, nutrients, or water availability between sites. In this context, it remains unknown whether specific factors (e.g., microclimate) that trigger tree growth, moth outbreaks, or tree survival can also affect SOC turnover rates, that is, a causal link between trees

and lower SOC stocks is not certain. This drawback can be overcome by investigating differences between living trees, dead trees, and treeless tundra on a small spatial scale of individual trees, thereby reducing the risk of confounding factors. On a small scale, Friggens et al. (2020) identified decreasing SOC stocks with distance from the tree, suggesting accumulation of organic matter close to trees, which opposes the conclusions based on comparisons of separate sites.

Here, we conducted a small-scale space-for-time approach on three independent sites by comparing SOC stocks and biochemical properties of soil under four tree statuses: living trees, dead trees (12 years since moth outbreak), dead trees (55 years since moth outbreak), and treeless tundra, which co-exist at the study sites. We hypothesized that (a) living trees have lower C stocks compared to treeless tundra. Such a negative net effect of a living tree could be caused by its N-demand, which stimulates SOM turnover to such an extent that it exceeds C input from the tree. Furthermore, because it is generally assumed that SOC decomposition slows down in the absence of trees and root exudates, we hypothesized (b) that tree death causes C stocks to develop toward the C stocks of the treeless tundra.

2 | MATERIALS AND METHODS

2.1 | Study area

The study area (69°9'N, 27°9'E, 130–156 m a.s.l.) is located in Northern Finnish Lapland, 12 km south of the village Nuorgam, approximately 5 km west of Lake Pulmankijärvi (Figure 1). The mean annual temperature was −1.6°C and mean annual precipitation was 448 mm during the time period 1981–2010, measured in Utsjoki, 35 km west of the study site (Finnish Meteorological Institute, 2020). Soils in this region are Podzols on sandy texture (WRB, 2015) and are not affected by permafrost.

The area is a heavily grazed year-round pasture of the Kaldoaivi reindeer herding cooperative. The herding of such semi-domesticated reindeer by the Sámi people has been practiced since centuries in this area (Kortesalmi, 2008). Reindeer densities in the Kaldoaivi area are around 2.38 reindeer/km² (2006–2007; Biuw et al., 2014). This density remained on average at a same level since the 1950s with the exception of two short-term drops in the late 1960s and mid 1970s and a short-term peak during the 1980s with 4.5 reindeer/km² (Biuw et al., 2014; statistics from the Reindeer Herders Association for reindeer numbers during 1960–2020). The trends in reindeer population densities are quite similar in the neighboring areas in Finland and in Norway, although the overall densities in Norway are slightly lower (i.e., 1.56 reindeer/km² in 2006–2007; Biuw et al., 2014). Traditionally, reindeer migrated between summer pastures in the coastal areas of the Arctic Ocean in Norway and winter pastures in the interior areas of Finland and Norway. Seasonal migration is still practiced in the neighboring areas in Norway. The contrasting year-round grazing in northernmost Finland results from the fact that seasonal reindeer migration is prevented by law since 1852 (Kortesalmi, 2008; Stark et al., 2021). Although rotational grazing on designated summer and winter pastures has been realized by means of fences in several Finnish districts, no such measures apply to the Kaldoaivi district (Biuw et al., 2014).

During the last century, the study area has been affected by two severe moth outbreak periods. The first occurred between 1960 and 1965, that is, approximately 55 years before sampling ("$dead_{55}$"); the second was between 2006 and 2008, that is, approximately 12 years before sampling ("$dead_{12}$"), as previously described (Kaukonen et al., 2013; Lehtonen & Heikkinen, 1995; Saravesi et al., 2015). Since some trees survived the respective outbreaks, the area is characterized by a mosaic that includes living trees (Figure 2a), dead but still standing trees ($dead_{12}$, Figure 2b), largely decomposed dead trees with only a stump remaining ($dead_{55}$, Figure 2c), and treeless tundra vegetation (Figure 2d).

We conducted a small-scale space-for-time substitution approach to investigate the effect of living trees, dead trees, and treeless tundra on SOC stocks and dynamics. Three independent sites were selected, each approximately 1 ha in size and located approximately 2 km away from each other. Criteria for selecting sites were that (a) all tree statuses (i.e., living, $dead_{12}$, and $dead_{55}$, treeless tundra) were present, each with several randomly distributed individuals, (b) the altitude of the sites was similar, and (c) the sites were located on a flat area to minimize differences in climate and microclimate between and within the sites. At each site, we selected four plots of each of the four tree statuses. Each plot had a size of 3.14 m², that is, 1 m radius around the tree or plot center, in the case of treeless tundra. Plots were chosen such that the next living or dead tree was at least 2 meters away.

2.2 | Understory vegetation

The percentage of understory vegetation cover was assessed at the species level by visual estimation within a circle of 1 m radius (Fenner, 1997). A few species were unidentifiable; these were grouped into the category of either "other grass species" or "other lichen species."

2.3 | Soil temperature and moisture

Between the beginning of July and end of September 2019, we measured soil temperature and volumetric water content (VWC) four times, parallel to the measurements of soil +understory respiration (see section 2.7). Soil temperature and VWC were measured at a depth of 5 cm. The VWC was measured at 5 locations around the respiration collar using a TDR sensor.

At each site, 2 plots per tree status were selected for temperature logging. Temperature loggers (Maxim iButton miniature temperature loggers, DS1922L) were buried at 10 cm depth and at 50 cm from the tree or plot center, in the case of treeless tundra. Temperature loggers were inserted at the end of July 2019, and remained in the soil for almost 1 year (with 13 days missing in July

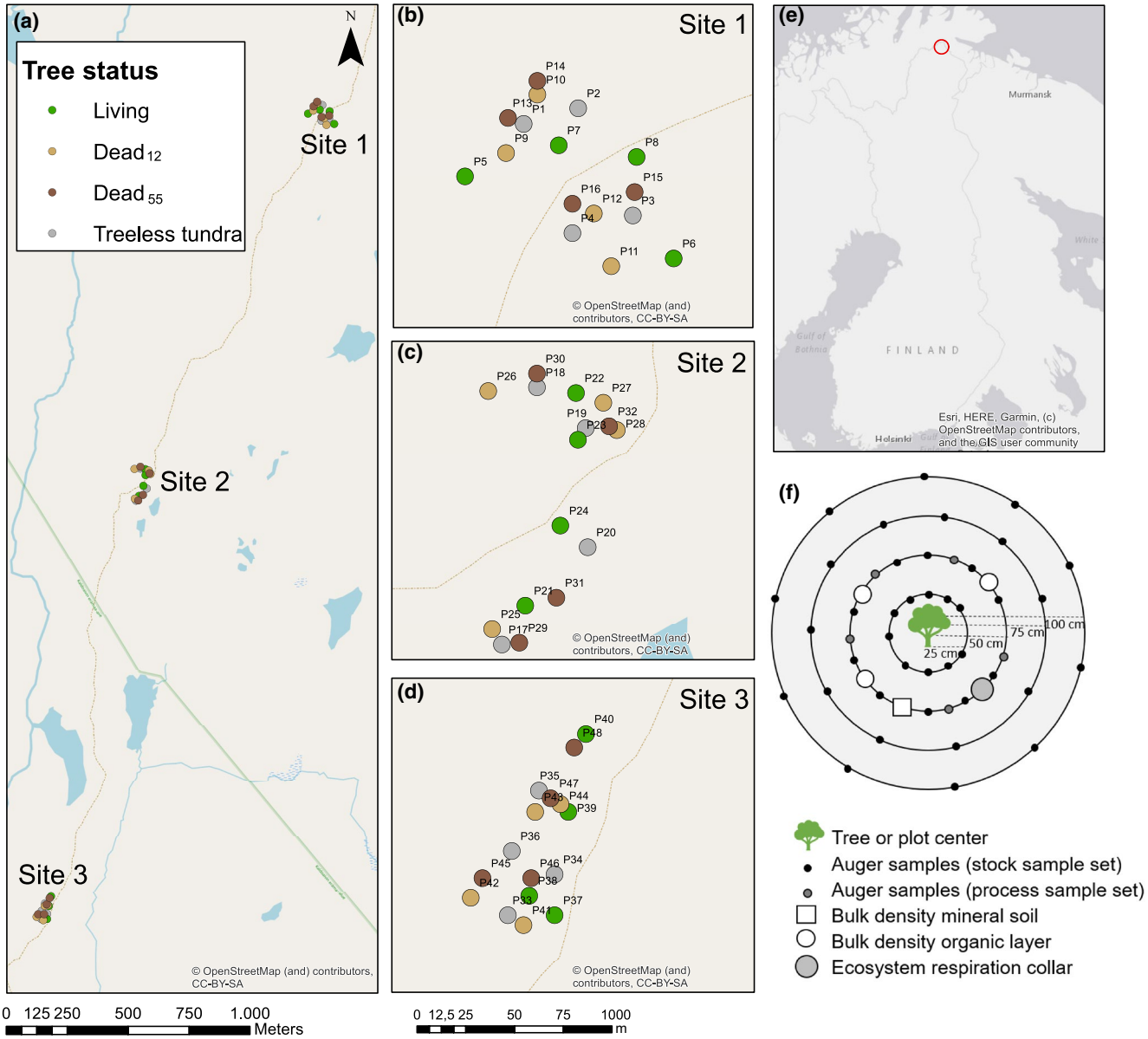

FIGURE 1 Location of the study sites and sampling design

2020) in plastic bags to prevent water damage. Temperature was recorded 4 times per day. The monthly mean temperature and the mean annual temperature were calculated for each plot.

2.4 | Aboveground and belowground plant carbon stocks

For living and dead$_{12}$ trees, we measured the height of the trunk and the diameter at breast height (DBH, at 1.3 m above ground). In case of bifurcation within the first 1.3 m, the DBH and height of each trunk were recorded separately. Using this data, we calculated aboveground biomass according to Starr et al. (1998).

For dead$_{55}$ trees, the height and diameter of the remaining stump were measured. Biomass of dead$_{55}$ trees was estimated according to Equation 1, where density was assumed to be $\rho = 478$ kg m^3, as reported for living trees of *B. pubescens* (Heräjärvi, 2004).

$$\text{Aboveground tree biomass}\,(kg) = \rho \times \pi \times r^2 \times h \quad (1)$$

Since the abovementioned equation applies to living trees, we corrected the biomass for density loss using annual decay rate constants of 4.5% upon tree death, which has been demonstrated for birch trees (Krankina & Harmon, 1995). Tree roots were estimated to be 29.2% of total tree biomass as suggested by Smith et al. (2016), that is, by dividing aboveground biomass by 70.8 and multiplying by 29.2. The proportion of carbon in all plant biomass pools was assumed to be 50% (Köster et al., 2015).

Understory aboveground biomass was calculated by harvesting all understory vegetation including moss and lichen from the respiration collars (20 cm diameter, see section 2.7, Figure 1f) at the end of the experiment. Plants were dried at 60°C and weighed. Assuming

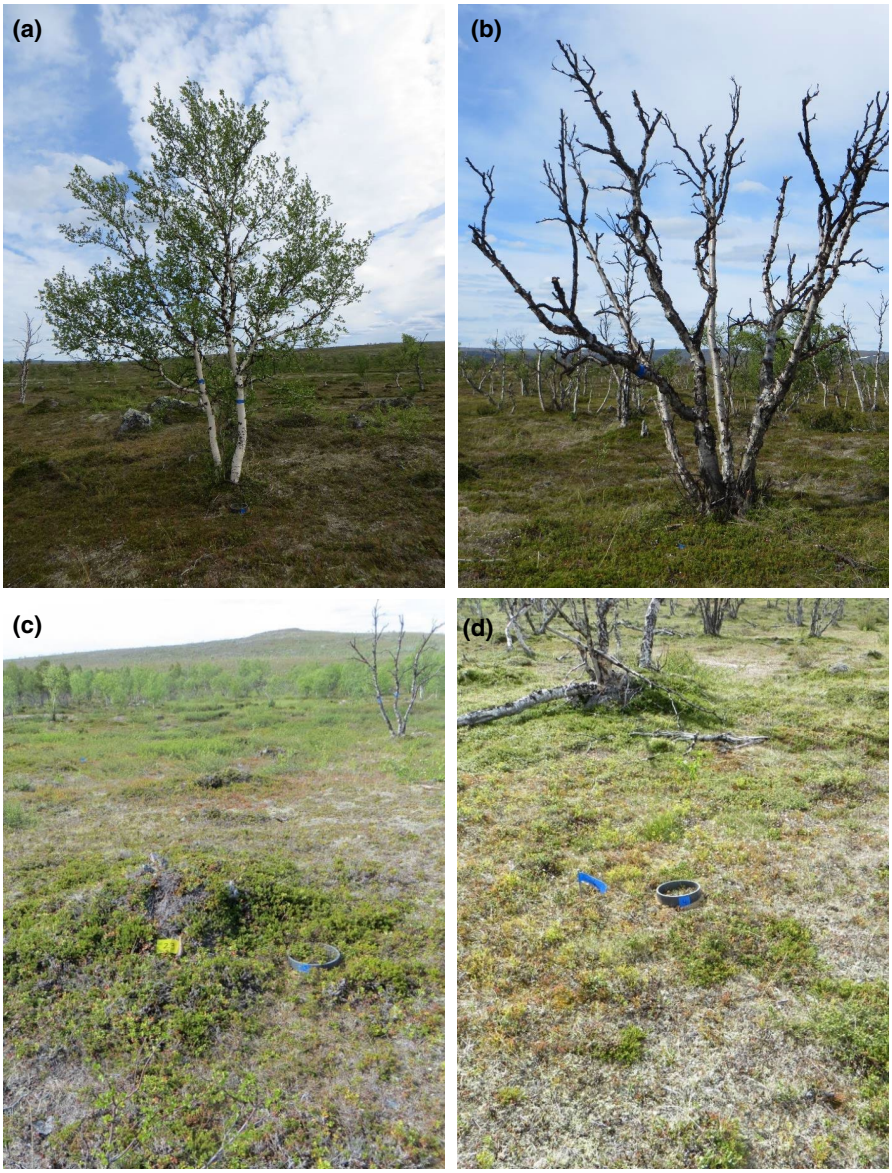

FIGURE 2 Pictures of tree status: (a) living tree, (b) $dead_{12}$ tree, (c) $dead_{55}$ tree, and (d) treeless tundra. Living and dead trees are scattered sparsely in the landscape

that vegetation inside the collars is representative of the entire plot, we extrapolated understory biomass to an area of 1 m radius around each tree or plot center. To determine understory root biomass, we took samples from 3 locations around each tree with an auger of 5 cm diameter (total organic layer +10 cm of mineral soil, see section 2.5; white circles in Figure 1f), and combined these to a composite sample per plot. Understory roots were isolated from the organic layer by sieving to 2 mm and subsequent washing. Such data were extrapolated to an area of 1 m radius around the plot center. C content was assumed to account for 50% of the biomass. The mineral soil contained no visible roots from understory vegetation.

2.5 | Determination of SOC stocks

To determine SOC stocks ("stock sample set," Figure 1f), 10 auger samples (2.5 cm diameter) were taken from 25, 50, 75, and 100 cm distance around the stem, or around the plot center in the case of treeless tundra (black dots in Figure 1f). The organic layer, the eluviated E horizon, and the illuviated B horizon up to a depth at which the auger could not be inserted any deeper (assuming that bedrock or large rocks were reached; cf. Parker et al., 2015) were taken separately. The thickness of each layer and the maximum depth of mineral soil were recorded for each of the 40 sampling points per plot. The auger samples were combined to form one composite sample from each distance and horizon per plot. Samples were dried at 40° immediately after sampling, subsequently sieved to 4 mm (organic) and 2 mm (mineral), and milled. The C and N contents were measured with VarioMax CN analyser (Germany). Since soils in this area are not calcareous (Hinneri et al., 1975) and our samples had a pH <6, the measured C contents were assumed to equal SOC.

Bulk density of the organic layer was measured at 3 locations 50 cm from each tree or plot center (white circles in Figure 1e) by drilling a sharp root auger (5 cm diameter) into the organic layer, measuring its thickness and resultant volume, and drying at 105°C. There was no obvious compression of the organic layer using the root auger. Bulk density of the mineral soil was determined by taking 1–2 soil cylinders

(170 cm^3) 50 cm from each tree or plot center. The volume of rock fragments >2 mm was subtracted from the cylinder volume to calculate bulk density of fine earth. To avoid error propagation, the average bulk density and stone content per site and tree status were used in calculations for organic layer and mineral soil, respectively. We are aware that soils also contain large rocks that were not included in the calculation of rock fragments from the soil cylinders. However, large rocks determined the maximum depth that could be sampled and were therefore included in the calculation of SOC stocks.

SOC stocks were calculated by Equation 2 and expressed as kg m^2.

$$\text{Stock}\left(\text{t ha}^{-1}\right) = \text{C content}\,(\%) \times \text{bulk density of fine earth}\left(\text{g cm}^3\right) \times \text{thickness}\,(\text{cm}) \times (1 - \text{rock fragments}\,[\%]\,/100) \quad (2)$$

To calculate overall stocks within a 1 m radius around a tree, SOC stocks were calculated for each distance separately, then multiplied with the respective area and summed, that is, we calculated total stocks within an area of 3.142 m^2. For the treeless tundra, stocks were calculated similarly around the center of the plot. Note that mineral soil was always sampled up to the bedrock. Hence, calculated stocks represent total stocks, but do not refer to a standardized depth. The maximum sampled depth was 70 cm of mineral soil, but such depths were only reached occasionally and not consistently within a given plot or distance around a tree. The average depth of mineral soil across all sites and plots was 6 cm.

Stocks of total soil N were calculated analogously to SOC stocks.

2.6 | Soil biological and chemical properties

For soil properties other than C and N stocks, we took samples 50 cm from the tree or plot center ("process sample set," small grey dots in Figure 1f). According to Parker et al. (2017), this is the distance at which the effect of tree status may be the greatest. At least 5 samples were taken from each plot using an auger (5 cm diameter). Additional samples were taken if collected soil material was not sufficient. We sampled the entire organic layer and the mineral soil up to 10 cm depth (i.e., composite of E and B layer). Samples were combined to form one composite sample per plot and soil layer (organic, mineral). Samples were kept in the fridge and sieved to 4 mm (organic) and 2 mm (mineral) within 1 week after sampling. Roots were removed, and samples were then split into separate bags and either dried (40°C), stored cold (8°C), or kept frozen (−20°).

Soil C and N contents were also measured as described above from dried soil for the process sample set.

Soil pH was measured from 1:2 soil-water slurry with a WTW electrode (Xylem Analytics, Germany).

Mineral N in the form of nitrate (NO_3^-) and ammonium (NH_4^+) was determined according to Carter and Gregorich (2008) from frozen soils after allowing the soil the thaw for 2 days. Mineral N was extracted from ~30 ml of soil with 100 ml 1 M KCl solution and analyzed by spectrophotometry (PerkinElmer—1420 VICTOR^{3}™, United States) according to Miranda et al. (2001). Mineral N content was calculated per g dry weight of soil.

For laboratory-based respiration measurements, frozen soils were thawed at 5°C for 2 days. An amount of soil corresponding to 8 g (organic) or 30 g (mineral soil) of dry weight was filled into incubation vessels, two replicates per sample, and subsequently rewetted to 50% of water-holding capacity (WHC) with distilled water, if necessary. Soil was pre-incubated at 20°C for 5 days. Basal respiration was then measured for 8 days, expressed as the average hourly CO_2 production per g soil or per g SOC, respectively. After measurement of basal respiration, glucose was added to each vessel at 8 mg glucose g^{-1} dry soil in aqueous solution (3.5 ml per vessel for organic layer, and 1.5 ml per vessel for mineral soil)—but not exceeding 60% WHC of soil. After the addition of glucose, soil respiration was measured for 100 h. This so-called substrate induced respiration (SIR) was originally developed to estimate the amount of microbial biomass in soils (Anderson & Domsch, 1978), but has subsequently often been used to assess microbial activities and characteristics (Blagodatsky et al., 2000). Here, we used it to determine microbial biomass carbon and investigate the degree of nutrient deficiency. According to Nordgren (1992), Meyer et al. (2017), and Meyer et al. (2018), mineralization of glucose depends on nutrient supply of microbes; hence, the potential to mineralize glucose serves as an indicator of nutrient availability to microbes. In mineral soil, we additionally tested whether N is the most limiting nutrient by subsequently adding 1.03 mg of $(NH_4)_2SO_4$ per g of soil (DIN ISO 17155 2012) in aqueous solution to one of the two incubation vessels per sample. Soil in the second incubation vessels received the same amount of water. If such N addition evokes an increase in CO_2 release, this would suggest that N was the most limiting nutrient and hindered the complete mineralization of glucose. We continued measuring CO_2 evolution for 2 days. The CO_2 production was measured using an automated respirometer that allows incubating 95 samples in parallel (Respicond, Nordgren Innovations AB, Sweden). The system provides a continuous measurement of CO_2 evolution by trapping CO_2 in potassium hydroxide (KOH) (Nordgren, 1988). Decrease in electrical conductivity in KOH solution caused by CO_2 entrapment was automatically measured every 60 min (basal respiration) or 30 min (after glucose addition) by platinum electrodes, and the changes in conductivity were automatically transformed to evolution rates based on Equation (3), where A is a conductivity constant that depends on the molarity of the KOH solution, C_{t0} is the conductance of the fresh KOH measured at the beginning of the incubation time, and C_{t1} is the conductance at time t.

$$CO_2 = A \times \left(C_{t0} - C_{t1}\right) / C_{t0} \quad (3)$$

We calculated the cumulative CO_2 evolution within 100 h after glucose addition (SIR_{cum}). Microbial biomass carbon (MBC) was derived from the maximum initial respiratory response according to Anderson and Domsch (1978) as follows:

$$\text{MBC}\left(\mu\text{g g}^{-1}\text{ soil}\right) = \left(\mu 1\ CO_2\ \text{g}^{-1}\text{ soil h}^{-l}\right) \times 40.04 + 0.37 \quad (4)$$

Enzyme activities were determined from thawed frozen soil. We measured the activities of cellobiosidase (EC 3.2.1.91), β-glucosidase

(EC 3.2.1.21), chitinase (EC 3.2.1.14), leucine amino-peptidase (EC 3.4.11.1), acid phosphatase (EC 3.1.3.2), β-xylosidase (EC 3.2.1.37), and N-acetyl-glucosaminidase using fluorometric substrates as described in Bell et al. (2013). Briefly, soil suspensions were obtained by mixing 2 g soil with 100 ml of 100 mM sodium acetate buffer (pH 5.5) in a mortar for 1 min. These soil suspensions were continuously stirred on a magnetic stirrer. A reaction mixture was prepared by mixing 200 μl of soil suspension with 50 μl of substrate in microplates (96 wells); for the blank, 200 μl of buffer and 50 μl of the respective substrate were used. All substrates were ordered from Sigma-Aldrich: 4-methylumbelliferyl β-D-cellobioside (substrate for cellobiosidase), 4-methylumbelliferyl D-glucopyranoside (β-glucosidase), 4-methylumbelliferyl-N-acetyl-β-D-glucosaminide (chitinase), leucine-aminomethylcoumarin (leucine amino-peptidase), 4-methylumbelliferyl phosphate acid (acid phosphatase), 4-methylumbelliferyl-β-D-xyloside (β-xylosidase). The plates were incubated for 140 min at room temperature (20°C) and enzymatic reactions were stopped by adding 10 μm 1 M NaOH, except for leucine-aminopeptidase. Fluorescence was measured with a plate reader (BMGLabtech, ClarioStar; excitation at 360 nm and emission at 460 nm). Quenched standard curves were built to each sample separately on 4-methylumbelliferone (MU), and 7-amino-4-methylcoumarin (AMC) for leucine amino-peptidase, by adding the same volume of soil slurry to each standard as was used in the enzyme activity assay. Enzymatic activities were expressed as nmol of MU/AMC per g^{-1} soil DW h^{-1}.

Additionally, we measured oxidative enzymes (phenol oxidase EC 1.14.18.1 and peroxidase EC 1.11.1.x) according to (Marx et al., 2001). A reaction mixture was prepared by adding 1 ml of soil suspension (prepared as above) to 1 ml of 20 mM DOPA solution (L-3,4-dihydroxyphenylalanin) in sodium acetate buffer (100 mM, pH 5.5). As a negative control, 1 ml of sodium acetate buffer and 1 ml of 20 mM DOPA solution were mixed; as blanks, 1 ml of sodium acetate buffer was mixed with 1 ml of soil suspension. Samples and blanks were shaken for 10 min and centrifuged (5 min, 2,000 g). Then, 250 μl of supernatants were dispensed into 96-well microplates. For peroxidase activity measurement, 10 μl of 0.3% H_2O_2 was added. After measurement of initial absorbance (450 nm), plates were incubated in darkness for 20 h at 20°C, and absorption was measured again. Enzymatic activities were expressed as nmol of DOPA g^{-1} soil DW h^{-1}.

2.7 | Soil +understory respiration

At a distance of 50 cm from each tree or plot center, we drilled a PVC collar (22 cm diameter) into the soil one week before the first measurement, by cutting roots and the organic layer with a knife, if necessary.

We measured soil +understory respiration four times during July–September 2019. soil +understory respiration in this study is defined as the sum of microbial, root, and understory vegetation respiration. We define the results as soil +understory respiration—not as ecosystem respiration—because aboveground respiration of trees was excluded in the measurements.

We placed a dark chamber (20 cm diameter, 25 cm height) on top of the collar, equipped with a fan to ensure ventilation. After closing the chamber, CO_2 concentration (ppm) was allowed to equilibrate for 1 min. The CO_2 concentration within the chamber was then recorded every minute for 5 min by a Vaisala GMP252 probe (Vaisala Oyj, Finland). The CO_2 accumulation rate (ppm min^{-1}) was calculated using a linear part of the recorded data, and CO_2 efflux F was calculated by Equation 5 where $\frac{dC}{dt}$ is the change in CO_2 concentration across measurement time (ppm min^{-1}), P is atmospheric pressure (in hPa, available from the nearest meteorological station in Nuorgam and adjusted for the ~100 m difference in elevation, Finnish Meteorological Institute, 2020), R is the gas constant (8.314 J mol^{-1} K^{-1}), T is the measurement temperature in Kelvin inside the chamber, V is the chamber volume in m^3 (0.009841 m^3), and A is the chamber area in m^2 (0.039761 m^2).

$$F\left(gCO_2cm^{-2}s^{-1}\right) = \frac{dC}{dt} \times \frac{P}{RT} \times \frac{V}{A} \times \frac{10^{-6}}{60} \times 44.01\frac{g}{mol} \quad (5)$$

Respiration measurements of each site were completed within 2 h such that the temperature and moisture conditions were similar for all plots within a site. The order of plots per site was randomized. Measurements of the three sites were taken within one day, except for the last measurement date when the duration of daylight was not sufficient.

2.8 | Statistics

We consider site as a block factor in ANOVA or random effect in linear mixed-effect models, respectively. We present treatment-specific mean values of the three sites in our figures. However, since the tree status appears to have different effects on soil properties at the three independent sites, we also discuss some site-specific differences, which are shown in the Supplementary material.

To investigate the effect of tree status on C stocks, C contents, and organic layer thickness, we used linear mixed-effect models for each soil layer (organic, E, B) separately, with tree status and distance to the tree as fixed effects and plot ID nested in site as a random effect. We also tested for interactions. If the tree status effect was significant, Tukey's honest significance test was applied to further investigate differences between each tree status. Data were checked for normality of residuals by visual inspection of qqplots, and variance homogeneity was tested with a Levene test. If assumptions were violated, the model was repeated on log- or square-transformed data. As this did not change the overall result, and because linear mixed-effect models have been shown to be robust to moderate violations of distributional assumptions (Schielzeth et al., 2020), we decided to keep the original model.

To compare the effect of tree status on overall SOC stocks within a 1 m radius around the tree or plot center, we multiplied the SOC stock (kg m^2) at each distance with the area of the respective distance radius and summed them. This was done for each soil layer separately, as well

as for total SOC stocks. We performed a one-way ANOVA with block design (site as block) and interaction term (tree status × site) for each soil layer separately (i.e., organic layer, E horizon, B horizon), as well as for total SOC stocks. Data were checked for normality of residuals with a Shapiro–Wilk test, and variance homogeneity was tested with a Levene test. If data were not normally distributed or did not reveal homogeneity of variances, they were log- or square-transformed.

To test for differences in soil +understory respiration between tree statuses, we performed a linear mixed-effect model with tree status, measurement date, soil temperature, and soil moisture as fixed effects, and plot ID nested in site as a random effect. We also tested for interactions. Non-significant interactions terms were removed from the model in a stepwise manner. Tukey's honest significance test was applied to further investigate differences between each tree status.

To test for differences in biochemical soil properties between tree statuses, we performed a one-way ANOVA with block design (site as block) for each soil layer (organic, mineral) separately. If effects were significant, a post-hoc Tukey's honest significance test was applied. If data were not normally distributed or did not reveal homogeneity of variances, they were log- or square-transformed.

Correlation analyses were conducted to explore relationships between the variables. In case of linear relationships and normal distribution of data, Pearson's correlation coefficient was used. Otherwise, Spearman's rank correlation coefficient was calculated.

Principal component analysis (PCA) was conducted to visualize relationships between the large number of measured variables and differences between sites and tree statuses. PCA was performed for the organic layer and mineral soil separately. All measured variables from the "process sample set" were included, except the large number of measured enzymes, which showed no correlation with tree status. We further included the soil +understory respiration rate at the middle of the growing season (12 July). The PCAs were performed in R using the function prcomp. Data were scaled to similar standard deviation and centered to a mean of zero. Ellipses are presented at a confidence interval of 90%.

If not otherwise stated, we define significant differences as $p < 0.05$.

Statistics and figures were performed in R (version 3.6.1, R Core Team, 2013) and maps in ArcGIS (version 10.8, Esri).

2.9 | Data

The data that support the findings of this study are openly available in Dryad (Meyer et al., 2021).

3 | RESULTS

3.1 | Understory vegetation cover

Understory vegetation was similar under living, $dead_{12}$, and $dead_{55}$ trees. The plant community of the treeless tundra differed considerably from that under living and dead trees. In the treeless tundra, moss (*Dicranum spp)*, lichen (*Ochrolechia frigida)*, and black crowberry (*Empetrum nigrum)* were most frequent, each covering around 30% of the area. Other species occurred occasionally. Under living, $dead_{12}$, and $dead_{55}$ trees, *Empetrum nigrum* accounted for 65–70% of the vegetation cover, that is, a considerably higher percentage than in treeless tundra. The remaining ~30% were mainly dominated by lingonberry (*Vaccinium vitis-idaea)*, *Dicranum spp*, and *Ochrolechia frigida*, each accounting for ~10% of the area (Figure S1).

3.2 | Soil temperature and moisture

The VWC that was measured four times between the beginning of July and end of September was on average higher at sites 2 and 3 in comparison with site 1, with significant differences in September but not in summer (Table 1). There was no significant effect of tree status on VWC.

Soil temperature at a depth of 10 cm was significantly affected by tree status: soils under living trees had lower average monthly temperatures in the summer compared with soil at the treeless tundra (Table 1). However, during the winter months, soils under living trees were on average warmer than at the treeless tundra sites, although this difference was not significant (Table 1, for details see also Figure S2). Hence, there was a significant tree status × month interaction (Table S1). At sites 1 and 3, summer temperatures under dead trees were intermediate between treeless tundra and living trees (significant tree status × site effect). On average, the soil temperatures at site 3 were lower throughout the years compared with sites 1 and 2 (Table 1).

3.3 | Aboveground and belowground carbon and nitrogen stocks

On average, the thickness of the organic layer was 5.5 ± 3.6 cm, but was significantly affected by tree status and site (Table 2, Figure 3a). Both living and dead trees had thicker organic layers than the treeless tundra. However, there was no consistent difference in organic layer thickness between living and dead trees: while site 1 revealed decreasing organic layer thickness in the order of living>$dead_{12}$=$dead_{55}$>treeless, $dead_{55}$ trees revealed the thickest organic layers at site 2 (Figure S3). At site 3, organic layer thickness was generally lower, with only small differences between tree status (Figure S3). Differences between tree status persisted up to at least 1 m from the tree, but decreased significantly with distance. Organic layer thickness did not change with distance to the plot center in the treeless tundra plots, yielding a significant tree status × distance interaction. C contents were also significantly higher under living and dead trees compared with the treeless tundra (Figure 3b). As a result, C stocks followed a similar pattern as organic layer thickness, with overall higher stocks under living and dead trees compared with the treeless tundra

TABLE 1 Temperature, soil moisture, and tree size characteristics across sites and tree statuses. Different lowercase letters indicate differences between sites (line by line) based on two factorial ANOVA. Different capital letters in the column "all sites" indicate differences between the tree statuses (two factorial ANOVA). In case of non-significant differences, letters were not provided

Tree status	Site 1	Site 2	Site 3	All sites
Living				
Tree height (m)	4.75 ± 0.6[a]	3.34 ± 0.5[b]	4.98 ± 0.7[a]	4.35 ± 0.91[A]
Aboveground tree biomass C (kg)	18.1 ± 7.1	8.7 ± 6.5	22.3 ± 7.2	16.3 ± 8.6[A]
Mean annual soil temperature (°C)[1]	2.26 ± 0.55	2.39 ± 0.42	1.95 ± 0.08	2.25 ± 0.38
Average temperature August	9.22 ± 0.02	9.27 ± 0.38	8.90 ± 0.37	9.13 ± 0.30[B]
Average temperature January	−0.76 ± 1.06	−0.79 ± 0.60	−0.74 ± 0.27	−0.76 ± 0.56
Volumetric water content July 12	21.8 ± 3.9	27.0 ± 9.7	22.6 ± 3.4	23.8 ± 6.2
Volumetric water content September 25	26.1 ± 5.7	36.5 ± 11.7	26.8 ± 5.0	29.8 ± 8.8
$Dead_{12}$				
Tree height (m)	4.33 ± 0.25	3.35 ± 0.72	3.36 ± 0.89	3.68 ± 0.78[B]
Aboveground tree biomass C (kg)	14.2 ± 14.4	8.1 ± 4.6	4.8 ± 4.5	9.1 ± 9.2[B]
Mean annual soil temperature (°C)	2.43 ± 0.58	2.09 ± 0.36	1.88 ± 0.61	2.13 ± 0.48
Average temperature August	9.71 ± 0.34	9.37 ± 0.04	9.12 ± 0.06	9.40 ± 0.31[AB]
Average temperature January	−0.91 ± 1.25	−1.27 ± 0.69	−1.23 ± 1.12	−1.14 ± 0.83
Volumetric water content July 12	19.6 ± 3.0	23.4 ± 4.9	19.9 ± 5.9	21.0 ± 4.7
Volumetric water content September 25	21.5 ± 5.6	29.7 ± 1.3	27.3 ± 4.4	26.2 ± 5.2
$Dead_{55}$				
Tree height (m)	0.18 ± 0.12	0.15 ± 0.04	0.25 ± 0.16	0.18 ± 0.11[C]
Aboveground tree biomass C (kg)	0.06 ± 0.04	0.03 ± 0.04	0.03 ± 0.03	0.04 ± 0.03[C]
Mean annual soil temperature (°C)	2.43 ± 0.20	2.25 ± NA	1.90 ± 0.20	2.18 ± 0.30
Average temperature August	9.52 ± 0.80	9.00 ± NA	9.24 ± 0.42	9.30 ± 0.50[AB]
Average temperature January	−0.73 ± 0.08	−0.49 ± NA	−0.95 ± 0.13	−0.77 ± 0.20
Volumetric water content July 12	20.8 ± 1.2	23.1 ± 7.3	23.5 ± 5.0	22.5 ± 4.8
Volumetric water content September 25	17.8 ± 2.7	28.2 ± 4.3	29.8 ± 2.3	25.3 ± 6.3
Treeless tundra				
Tree height (m)	NA	NA	NA	NA
Aboveground tree biomass C (kg)	NA	NA	NA	NA
Mean annual soil temperature (°C)	2.27 ± 0.49	2.35 ± 0.09	2.00 ± 0.19	2.20 ± 0.29
Average temperature August	9.94 ± 0.12	9.60 ± 0.29	9.44 ± 0.05	9.66 ± 0.27[A]
Average temperature January	−1.48 ± 1.00	−0.64 ± 0.02	−0.89 ± 0.28	−1.00 ± 0.60
Volumetric water content July 12	23.7 ± 2.6	21.2 ± 1.8	28.4 ± 8.3	24.4 ± 5.6
Volumetric water content September 25	20.4 ± 3.7	29.2 ± 1.1	34.0 ± 3.7	27.9 ± 6.5
All tree statuses				
Mean annual soil temperature (°C)	2.35 ± 0.37	2.27 ± 0.26	1.93 ± 0.26	2.18 ± 0.35
Average temperature August	9.60 ± 0.43[a]	9.35 ± 0.29[ab]	9.17 ± 0.30[b]	9.38 ± 0.38
Average temperature January	−0.97 ± 0.80	−0.84 ± 0.49	−0.95 ± 0.49	−0.92 ± 0.59
Volumetric water content July 12	21.5 ± 3.0	23.7 ± 6.3	23.6 ± 6.2	22.9 ± 5.4
Volumetric water content September 25	21.5 ± 5.1[b]	30.9 ± 6.6[a]	29.5 ± 4.6[a]	27.3 ± 6.8

[1]Excluding data for 13 days in July where measurements were not available.

(Figure 3c). This effect similarly decreased with increasing distance from the tree, and high variability between sites was seen (Figure S3).

The average thickness of the E horizon was 2.1 ± 0.8 cm across all sites, tree status, and distances from a tree. The remaining mineral soil up to the bedrock ("B horizon") was on average 4.1 ± 3.3 cm thick. In mineral soil, neither the thickness, SOC contents nor SOC stocks were significantly different between tree statuses (Table 2). There was no clear trend with distance from the tree (Table 2, see also Figures S4 and S5).

TABLE 2 F and P statistics of the effects of tree status and distance on layer thickness, C contents, and C stocks

	Numerator degrees of freedom	Denominator degrees of freedom	F-value	*p*-value
Thickness organic layer				
Intercept	1	140	29.17994	<0.0001
Tree status	3	42	6.02882	0.0016
Distance	1	140	83.16632	<0.0001
Tree status x distance	3	140	6.94514	0.0002
Tukey's Post-hoc test: Living[b], $dead_{12}$[ab], $dead_{55}$[b], no tree[a]				
C contents organic layer				
Intercept	1	140	2648.2521	<0.0001
Tree status	3	42	3.1389	0.0352
Distance	1	140	0.0068	0.9342
Treatment x distance	3	140	4.7418	0.0035
Tukey's Post-hoc test: Living[ab], $dead_{12}$[ab], $dead_{55}$[b], no tree[a]				
C stock organic layer				
Intercept	1	140	20.76419	<0.0001
Tree status	3	42	4.52700	0.0077
Distance	1	140	66.57137	<0.0001
Tree status x distance	3	140	7.42310	0.0001
Tukey's Post-hoc test: Living[ab], $dead_{12}$a[ab], $dead_{55}$[b], no tree[a]				
Thickness E horizon				
Intercept	1	140	148.00668	<0.0001
Tree status	3	42	1.17097	0.3322
Distance	1	140	0.17918	0.6727
Tree status x distance	3	140	0.91127	0.4373
Tukey's Post-hoc test: Living[a], $dead_{12}$[a], $dead_{55}$[a], no tree[a]				
C contents E horizon				
Intercept	1	140	213.33624	<0.0001
Tree status	3	42	1.36516	0.2665
Distance	1	140	1.72383	0.1913
Tree status x distance	3	140	1.92226	0.1287
Tukey's Post-hoc test: Living[a], $dead_{12}$[a], $dead_{55}$[a], no tree[a]				
C stock E horizon				
Intercept	1	140	44.89496	<0.0001
Tree status	3	42	1.85612	0.1518
Distance	1	140	0.22089	0.6391
Tree status x distance	3	140	2.25095	0.0851
Tukey's Post-hoc test: Living[a], $dead_{12}$[a], $dead_{55}$[a], no tree[a]				
Thickness B horizon				
Intercept	1	140	11.034098	0.0011
Tree status	3	42	1.310010	0.2838
Distance	1	140	1.731523	0.1904
Tree status x distance	3	140	1.525913	0.2105
Tukey's Post-hoc test: Living[a], $dead_{12}$[a], $dead_{55}$[a], no tree[a]				
C contents B horizon				
Intercept	1	139	52.37210	0.1610
Tree status	3	42	1.08981	0.3639

TABLE 2 (Continued)

	Numerator degrees of freedom	Denominator degrees of freedom	F-value	*p*-value
Distance	1	139	1.49864	0.2230
Tree status x distance	3	139	0.41035	0.7458
Tukey's Post-hoc test: Living[a], $dead_{12}$[a], $dead_{55}$[a], no tree[a]				
C stock B horizon				
Intercept	1	139	22.972520	<0.0001
Tree status	3	42	1.338915	0.2746
Distance	1	139	0.095715	0.7575
Tree status x distance	3	139	3.352526	0.0209
Tukey's Post-hoc test: Living[a], $dead_{12}$[a], $dead_{55}$[a], no tree[a]				

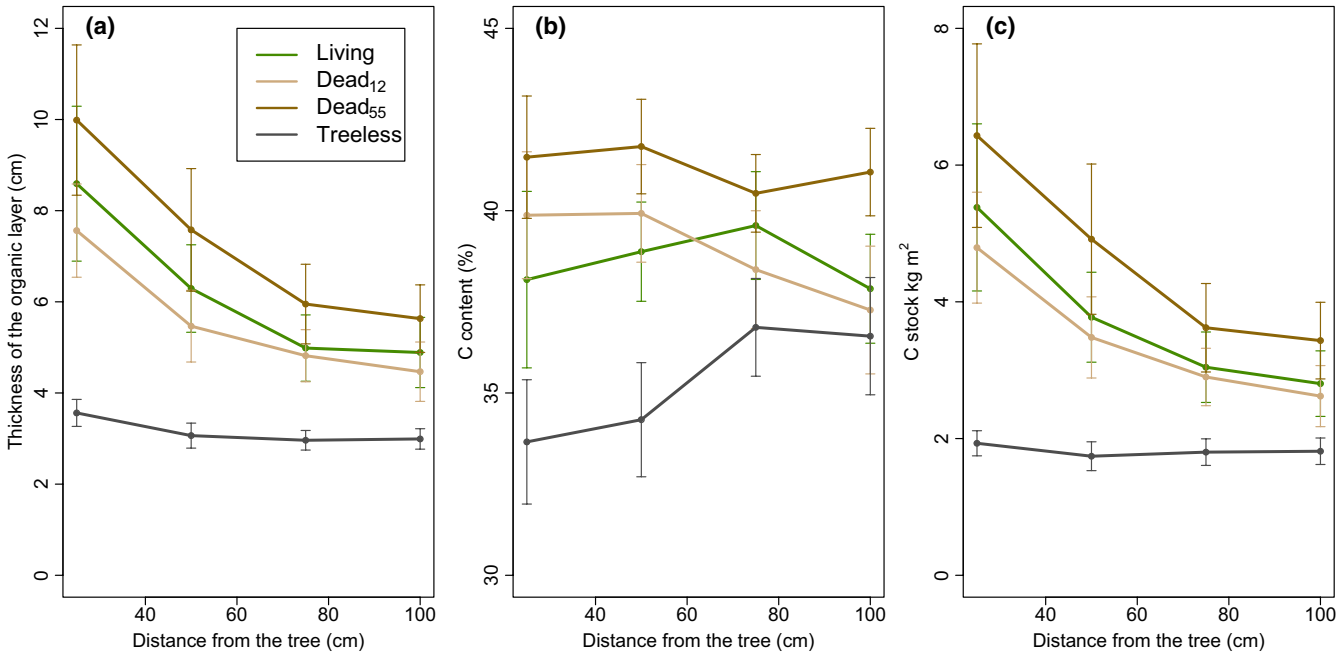

FIGURE 3 Thickness (a), C contents (b), and C stocks (c) of the organic layer. Mean and standard error are presented

Total overall SOC stocks within 1 m distance (i.e., sum of SOC stocks from org + E + B, Figure 4) decreased in the order of $dead_{55}$>living> $dead_{12}$>treeless, with significant differences only between treeless tundra and living trees and between treeless tundra and $dead_{55}$ (Figure 4).

Overall ecosystem C stocks decreased in the order of living>$dead_{12}$>$dead_{55}$>treeless tundra (Figure 4) and were mainly driven by changes in aboveground biomass, which significantly decreased upon tree death, especially at later stages.

Soil N stocks were also calculated (see supplementary information). Across all distances and sites, average N stocks in the organic layer were 0.118 ± 0.077 kg m^2 (living), 0.105 ± 0.062 kg m^2 ($dead_{12}$), 0.130 ± 0.084 kg m^2 ($dead_{55}$), and 0.056 ± 0.023 kg m^2 (treeless tundra). In the E layer, average N stocks were 0.078 ± 0.035 kg m^2 (living), 0.080 ± 0.029 ($dead_{12}$), 0.087 ± 0.040 kg m^2 ($dead_{55}$), and 0.048 ± 0.026 kg m^2 (treeless tundra). In the B layer, average N stocks were 0.187 ± 0.129 kg m^2 (living), 0.126 ± 0.092 kg m^2 ($dead_{12}$), 0.150 ± 0.133 kg m^2 ($dead_{55}$), and 0.155 ± 0.131 kg m^2 (treeless tundra). For site- and distance-specific N contents and N stocks, see Figures S6–S8.

3.4 | Ex-situ soil respiration measurement

Basal respiration measured under standardized conditions of moisture (50% of WHC) and temperature (20°C) decreased in the order of living>$dead_{12}$=$dead_{55}$> treeless tundra, both in the organic (Figure 5a) and mineral layer (Figure 5f). The effect of tree status was significant in mineral soil, but only close to significant (p = 0.09) in the organic layer. A post-hoc test revealed significant differences in mineral soil only between living trees and the treeless tundra (Figure 5f). Although dead trees were not significantly different from living trees or the treeless tundra, there was a tendency that dead trees were in transition between living trees and treeless

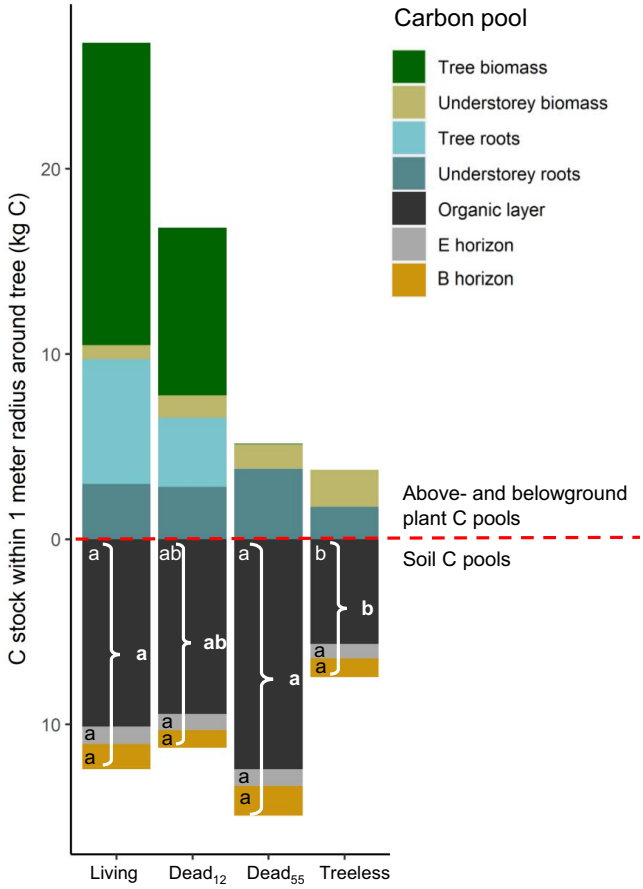

FIGURE 4 Total C stocks averaged over the three sites for the investigated area of 1 m radius around a tree or plot center of the treeless tundra (3.14 m²). Soil was sampled up to the bedrock, that is, total SOC stocks were measured. Letters indicate significance differences of soil C pools

tundra, both in mineral soil and organic layer (Figure 5a,f). The soil respiration rate was related to C contents in mineral soil (r = 0.55, $p < 0.001$) but not in the organic layer (r = 0.15, $p = 0.31$). When expressed per g of C (i.e., SOC-specific respiration), soil respiration was not significantly different between each tree status, neither in the organic layer nor in the mineral soil (Figure 5b,g). The SOC-specific respiration was inversely related to the C/N ratio in the organic layer (r = −0.61, $p < 0.001$) and mineral soil (r = −0.44, $p < 0.001$).

Following the addition of glucose, hourly CO_2 release increased in comparison with basal respiration rate (Figure S9). The cumulative amount of CO_2 released within 100 h after glucose addition (i.e., SIR_{cum}) decreased in the order of living >$dead_{12}$=$dead_{55}$> treeless tundra, both in the organic layer (Figure 5c) and in mineral soil (Figure 5h). The effect of tree status was significant. Post-hoc tests revealed that SIR_{cum} under living trees, $dead_{12}$, and $dead_{55}$ trees differed significantly from the treeless tundra in the organic layer. In mineral soil, only living trees differed from the treeless tundra. There was a tendency for dead trees to differ from living trees and from the treeless tundra, although these differences were not significant. SIR_{cum} was positively related to the concentrations of NO_3, both in the organic layer (r = 0.30, $p = 0.04$) and in mineral soil (r = 0.35, $p = 0.02$). Adding $(NH_{4)2}SO_4$ to the glucose-amended mineral soil induced larger CO_2 release than without N addition (Figure S9).

3.5 | Soil biological and chemical properties

Neither the pH value, C/N ratios, nor enzyme activities differed significantly between tree status (Table 3). Moreover, the microbial biomass (MBC) did not differ significantly between tree status in the organic layer and mineral soil (Figure 5d,i), although there was a decreasing trend in the order of living>$dead_{55}$>$dead_{12}$>treeless tundra (Figure 5i).

Soil N availability differed across tree status: in the organic layer, NO_3^- concentrations were significantly higher under living trees than under $dead_{55}$ and the treeless tundra; $dead_{12}$ was intermediate, although these differences were not significant (Figure 5e). This difference did not persist in mineral soil, where no significant differences were found due to the overall low NO_3^- content (Figure 5j). In all plots, NH_4^+ dominated the soil mineral N pool with a minimum of 80% (Table 3), but did not differ significantly between tree status, neither in the organic layer nor in mineral soil.

3.6 | Soil +understory respiration

Soil +understory respiration was significantly higher under living and dead trees compared with the treeless tundra, but there was no significant difference between living and dead trees (Table 4, Figure 6). Nevertheless, there were remarkable difference between tree status among the three sites (Figure S10). At site 1 and site 3, average soil +understory respiration decreased in the order of living>$dead_{12}$>$dead_{55}$>treeless tundra. However, at site 2, $dead_{55}$ revealed the highest ecosystem respiration rates, even exceeding those of living trees.

3.7 | Principal component analysis

In the organic layer, the first and second principal components explained 31% and 27% of variance, respectively (Figure 7a). PC1 was significantly correlated ($p < 0.05$) with the original variables: thickness of the organic layer (r = −0.87), SOC stock (r = −0.85), C contents (r = −0.89), C/N ratio (r = −0.70), and SOC-specific respiration (r = 0.75), that is, with variables related to SOC quantity and quality. PC2 was significantly correlated with NO_3^- (r = −0.48), NH_4^+ (r = −0.36), N (r = −0.62), MBC (r = −0.70), SIR_{cum} (r = −0.88), soil +understory respiration (r = −0.45), and soil respiration (r = −0.89), that is, with variables related to N availability and microbial activity. Soil from treeless tundra was separated from living trees mainly along PC2, where treeless tundra revealed higher values, that is, lower N availability and microbial activity than living trees. Dead trees were intermediate between living trees and treeless tundra. The soil properties in treeless tundra mainly varied along the second component, whereas living trees varied along the first component, that is, the PCA ellipse showing the 90% confidence interval of living trees was at a 45° angle to the ellipse of

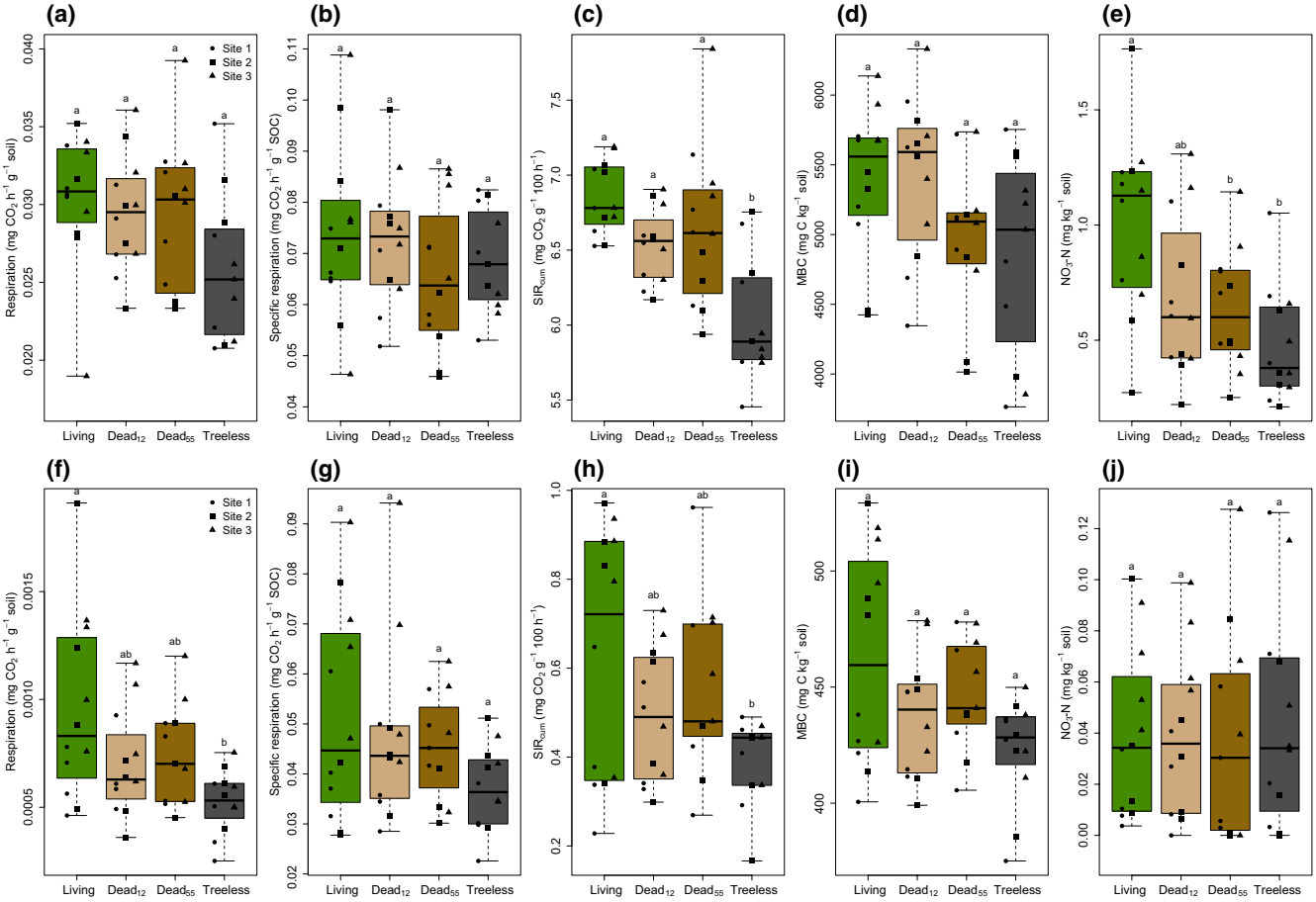

FIGURE 5 Effect of tree status on soil properties in the organic layer (upper row) and mineral soil (lower row). Whiskers show the minimum and maximum value, respectively. (a) Soil respiration (organic layer), (b) SOC-specific respiration (organic layer), (c) cumulative CO_2 evolution within 100h after glucose addition (organic layer), (d) microbial biomass (organic layer), e) NO_3-N (organic layer), (f) soil respiration (mineral soil), g) SOC-specific respiration (mineral soil), (h) cumulative CO_2 evolution within 100h after glucose addition (mineral soil), (i) microbial biomass (organic layer), and (e) NO_3-N (mineral soil). In each figure, different letters indicate significant differences ($p<0.05$). Different symbols indicate the distribution at the three sites

dead trees (Figure 7a), which were also immediate here. Furthermore, living and dead trees revealed larger variability in the multidimensional space, while treeless tundra clustered in a smaller area.

In mineral soil, the first and second principal components explained 34% and 19% of variance, respectively (Figure 7b). There was no clear clustering by tree status. As already observed for the organic layer, living trees revealed the largest variability in the multidimensional space, while treeless tundra clustered in a smaller area, with dead trees in between.

4 | DISCUSSION

In this study, we aimed to understand the effect of treeline advance and decline on SOC stocks and dynamics. To this end, we compared SOC stocks and biochemical soil properties under living trees, treeless tundra, and two stages of dead trees (12 and 55 years since moth outbreak) in a small-scale space-for-time approach. In summary, our first hypothesis (section 4.1) of living trees having lower C stocks compared to treeless tundra was rejected. Contrary to our hypothesis, the net effect of the living tree on soil C stocks was positive. However, this does not exclude the possibility that the living tree enhances SOM decomposition via priming effects. In fact, some of our results point toward higher priming effects under living trees, but the net effect of the tree was positive, which means that the C losses from accelerated SOM decomposition under living trees did not exceed the C inputs. Our second hypothesis (section 4.2) was that tree death causes the C stocks to develop toward the C stocks of the treeless tundra. Indeed, several soil properties under dead trees were in transition between those of living trees and treeless tundra. Yet, this did not apply to SOC stocks, which remained at an elevated level comparable to that of living trees, even 55 years after the moth outbreak. Hence, also our second hypothesis was rejected.

4.1 | Effect of living birch trees on ecosystem carbon stocks and soil organic matter turnover

Assuming that priming is a relevant mechanism under living trees, we hypothesized that accelerated SOC turnover leads to smaller SOC

TABLE 3 Soil properties in 50 cm distance from the tree or plot center, respectively

		Organic				Mineral soil			
		Living	$Dead_{12}$	$Dead_{55}$	Treeless	Living	$Dead_{12}$	$Dead_{55}$	Treeless
SOC	%	42.2 ± 6.9^{ab}	41.1 ± 5.5^{ab}	45.4 ± 4.4^{a}	37.9 ± 6.1^{b}	2.13 ± 1.57^{a}	1.57 ± 0.64^{a}	1.67 ± 0.47^{a}	1.41 ± 0.19^{a}
N	%	1.31 ± 0.14^{a}	1.31 ± 0.11^{a}	1.38 ± 0.18^{a}	1.21 ± 0.22^{a}	0.069 ± 0.036^{a}	0.059 ± 0.024^{a}	0.062 ± 0.018^{a}	0.059 ± 0.011^{a}
C/N		32.0 ± 2.7^{a}	31.4 ± 2.5^{a}	33.2 ± 4.4^{a}	31.5 ± 2.5^{a}	30.2 ± 7.0^{a}	27.9 ± 9.4^{a}	28.6 ± 9.8^{a}	24.2 ± 1.5^{a}
NH_4-N	mg NH_4-N kg^{-1}	12.30 ± 8.72^{a}	7.99 ± 3.29^{a}	15.89 ± 12.00^{a}	9.75 ± 4.72^{a}	0.96 ± 0.73^{a}	0.76 ± 0.55^{a}	0.93 ± 1.21^{a}	1.09 ± 1.06^{a}
NO_3-N	mg NO_3-N kg^{-1}	1.01 ± 0.39^{a}	0.68 ± 0.35^{ab}	0.63 ± 0.26^{b}	0.47 ± 0.24^{b}	0.04 ± 0.03^{a}	0.04 ± 0.03^{a}	0.04 ± 0.04^{a}	0.04 ± 0.04^{a}
pH		4.17 ± 0.21^{a}	4.16 ± 0.19^{a}	4.00 ± 0.19^{a}	4.04 ± 0.15^{a}	5.50 ± 0.26^{a}	5.61 ± 0.34^{a}	5.49 ± 0.28^{a}	5.51 ± 0.29^{a}
β-glucosidase	nmol activity g^{-1} h^{-1}	114.02 ± 95.16^{a}	76.55 ± 145.88^{a}	33.17 ± 27.94^{a}	64.44 ± 61.80^{a}	NA	NA	NA	NA
Leucine aminopeptidase	nmol activity g^{-1} h^{-1}	0.013 ± 0.031^{a}	0.019 ± 0.029^{a}	0.002 ± 0.008^{a}	0.006 ± 0.010^{a}	NA	NA	NA	NA
N-acetyl-glucosaminidase	nmol activity g^{-1} h^{-1}	340.1 ± 262.2^{a}	210.1 ± 138.3^{a}	300.5 ± 117.4^{a}	262.0 ± 156.9^{a}	NA	NA	NA	NA
Phosphatase	nmol activity g^{-1} h^{-1}	1800 ± 1261^{a}	1768 ± 999^{a}	1539 ± 798^{a}	2686 ± 1172^{a}	NA	NA	NA	NA
Cellobiosidase	nmol activity g^{-1} h^{-1}	98.7 ± 62.2^{a}	64.7 ± 34.1^{a}	90.8 ± 33.9^{a}	67.7 ± 64.1^{a}	NA	NA	NA	NA
β-xylosidase	nmol activity g^{-1} h^{-1}	155.2 ± 71.3^{a}	116.2 ± 81.1^{a}	148.8 ± 60.1^{a}	169.2 ± 115.4^{a}	NA	NA	NA	NA
Peroxidase	nmol activity g^{-1} h^{-1}	0.12 ± 0.28^{a}	0.66 ± 0.95^{a}	0.27 ± 0.43^{a}	0.23 ± 0.27^{a}	NA	NA	NA	NA
Phenoloxidase	nmol activity g^{-1} h^{-1}	0.050 ± 0.12^{a}	0.042 ± 0.077^{a}	0.171 ± 0.328^{a}	0.064 ± 0.151^{a}	NA	NA	NA	NA

Note: In each row, different letters indicate significant differences (tested for organic and mineral separately).

TABLE 4 F and P statistics for ecosystem respiration measurements. Significant effects are highlighted in bold

Ecosystem respiration	Numerator degrees of freedom	Denominator degrees of freedom	F-value	*p*-value
Intercept	1	129	213.62159	<0.0001
Tree status	3	39	3.81693	**0.0172**
Measurement date	1	129	31.37610	**<0.0001**
Soil moisture	1	129	1.05691	0.3058
Soil temperature	1	129	160.21566	**<0.0001**
Measurement date x soil temperature	1	129	61.13878	**<0.0001**
Tukey's Post-hoc test: Living[b], $dead_{10}$[ab], $dead_{60}$[ab], no tree[a]				

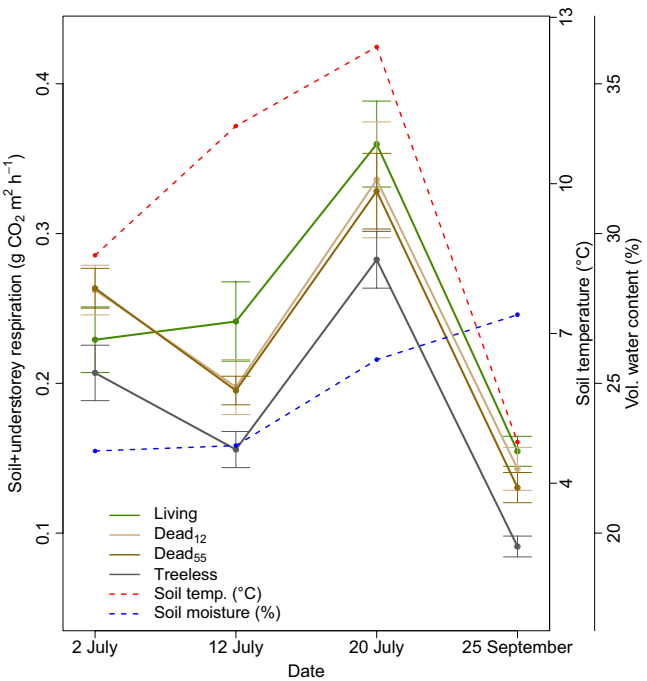

FIGURE 6 Soil +understory respiration, soil temperature, and volumetric soil water content. Mean and standard error are presented

stocks under living trees compared to treeless tundra (Hartley et al., 2012; Parker et al., 2015; Wilmking et al., 2006). Contrary to this hypothesis, we found that SOC stocks were on average significantly higher under living trees compared with treeless tundra (Figure 3c). Higher SOC stocks were still evident even 1 m from the tree, although these differences decreased with increasing distance. Most studies that have reported lower SOC stocks under living trees have compared forested sites with separate treeless sites, for example, along latitudinal or altitudinal transects or at locations with considerable distance between each other. In such approaches, SOC stocks could be also affected by differences in temperature, moisture conditions, soil characteristics, and/or aboveground and belowground litter input (e.g., Rapalee et al., 1998; Sjögersten & Wookey, 2004). In this regard, a causal link between trees and lower SOC stocks is not certain. With our single tree scale approach, we could investigate the effect of trees under otherwise rather similar conditions. Based on a similar approach, Friggens et al. (2020) identified decreasing SOC stocks with increasing distance from trees, and thus a positive effect of trees on SOC stocks. Similarly, Adamczyk et al. (2019) showed that priming-induced SOC losses are smaller than the positive effect of tree roots on SOC formation and stabilization. It therefore seems likely that living trees can also accumulate SOM in subarctic soils, that is, that trees have a positive net effect on SOC stocks. Together with the large aboveground C storage shown here (Figure 4) and elsewhere (Heliasz et al., 2011), our results imply that living trees could strengthen the C sink of the ecosystem.

The effect of living trees on SOC stocks decreased with soil depth. Even if the average SOC stocks in the E and B horizon were higher under living trees compared with treeless tundra (Figure 4), this difference was not statistically significant considering the large variability (Table 2; Figures S3 and S4). Thus, the significant differences in SOC stocks between living trees and treeless tundra (Figure 4) were mainly driven by the thickness and C concentrations of the organic layer. It is surprising that the effect of living trees does not persist with depth, as Ding et al. (2019) observed 46% of birch fine root biomass was located in mineral soil, which may lead to considerable C inputs. It is possible that priming effects by root exudates resulted in faster mineralization of SOM in the N-poor mineral soil under living trees. Hartley et al. (2010), Karhu et al. (2016), and Wang et al. (2015) also found that positive priming mainly takes place in the mineral soil, but not or at lower rates in the organic layer. Hence, the effect of higher SOC input under living trees may be cancelled out by priming in mineral soil.

Numerous studies have clearly demonstrated that priming effects occur in the field under living trees (Adamczyk et al., 2019; Clemmensen et al., 2021; Hartley et al., 2012; Parker et al., 2015). Although we did not directly measure priming, we have several results that point toward accelerated SOM decomposition under living trees at our study sites, as discussed in detail below.

Since priming is notoriously difficult to measure under field conditions, it is often investigated in incubation experiments after the addition of ^{13}C labeled substrates, which allows native SOC mineralization to be distinguished from mineralization of labile C (Karhu et al., 2016). Such experiments only indicate a potential priming effect under standardized C supply, but do not reflect the naturally occurring priming intensity in soil where labile C supply varies between living trees, dead trees, and treeless tundra. Yet, priming has been reported to be driven by microbial N mining, that is, by microbial

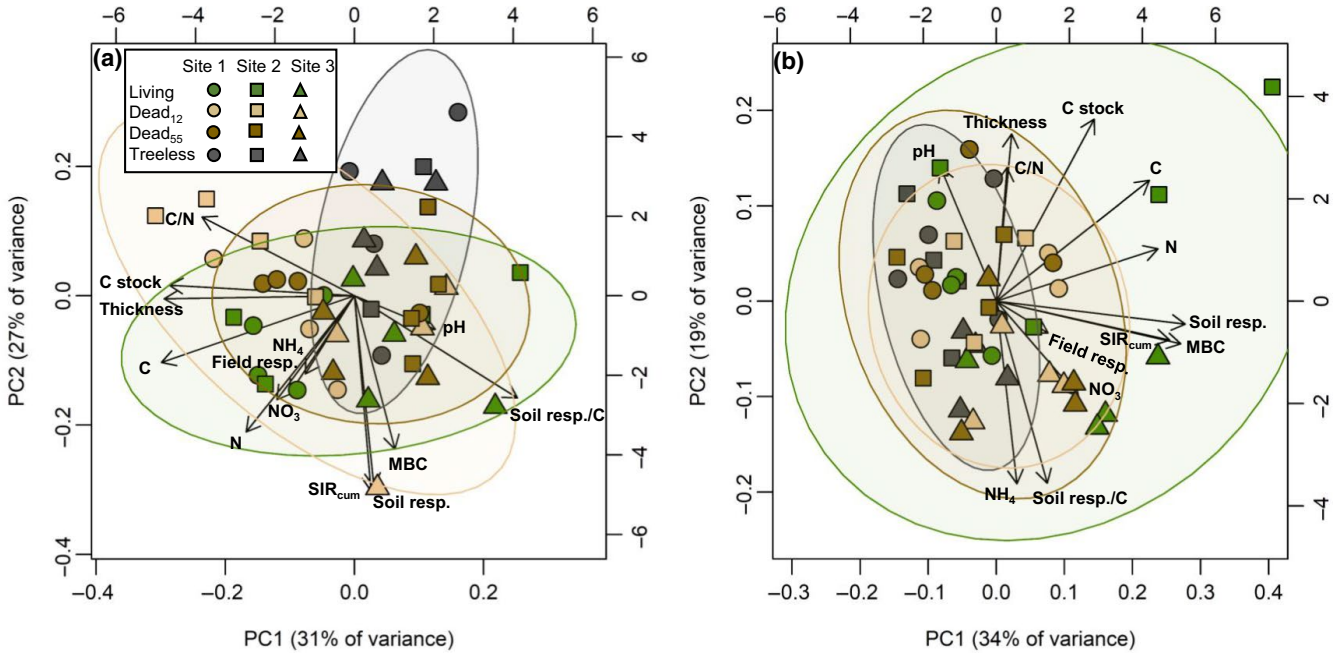

FIGURE 7 Principal component analysis of (a) organic layer and (b) mineral soil. Principal component scores of samples are represented by symbols, and loadings of variables are represented by vectors. Increasing vector distance from the plot center reflects a stronger influence on the respective principal component. The angle between vectors indicates the correlation between variables: a small angle indicates a positive correlation, a 90°C vector indicates no correlation, and diverging vectors (i.e., 180°C) indicate negative correlations. Ellipses show the 90% confidence interval for the respective tree status. Thickness refers to the thickness of the organic layer or mineral soil, respectively; C and N refer to concentrations (%); C stock is the calculated SOC stock at 50 cm distance; Soil resp./C is the SOC-specific respiration rate; SIR_{cum} is the cumulative CO_2 evolution within 100 h after glucose addition; Soil resp. is the soil respiration rate under laboratory conditions; Field resp. is soil +understory respiration measured in the field; and MBC is microbial biomass carbon

decomposition of SOM for N acquisition (Chen et al., 2014; Fontaine et al., 2011). In this context, Bengtson et al. (2012) and Dijkstra et al. (2009) pointed out that N mineralization and priming are coupled: labile C supply (e.g., from fresh litter and root exudates) increases microbial N demand, eventually increasing the activity of extracellular enzymes that decompose SOM for N acquisition. Hence, mineral N contents may provide hints for priming. Indeed, we found higher NO_3^- contents under living trees compared with treeless tundra. The finding of higher N availability under living trees was also corroborated by incubation experiments after adding glucose: soils taken under living trees were able to mineralize larger amounts of glucose, which, according to Nordgren (1992) and Meyer et al. (2018) suggests higher amounts of available nutrients, in this case N (as tested by N additions, Figure S9). Other studies have also shown that living birch trees increase soil N availability (Mikola et al., 2018; Silfver et al., 2020). We interpret this finding as an indicator of N mining, which is presumably coupled with accelerated turnover of SOM, that is, with priming. However, higher mineral N contents may also be interpreted inversely: higher mineral N contents under living trees may indicate less need of microbes to decompose SOM for N acquisition (Craine et al., 2007), that is, it suppresses priming. In light of the very N-poor subarctic soils (Hicks et al., 2020), it seems contradictory to find an excess of mineral N despite the greater N demand of birch roots. Hence, the excess mineral N under living trees most likely results from accelerated SOM decomposition close to the tree. This is further indicated by largest soil +understory respiration rates and microbial biomass under living trees.

Besides higher mineral N contents, we also found elevated N stocks under living trees than under treeless tundra. As both C and N are major components of SOM, higher N stocks under living trees are not necessarily surprising, since SOC stocks were also high. In such nutrient-limited regions, it is unlikely that the soil beneath the tree contained sufficient N for accumulating such high amounts of aboveground and belowground organic matter stocks. While larger mineral N contents can be explained by accelerated SOM decomposition close to the tree, another mechanism must be responsible for elevated N stocks. Although N fixation might be a potential source of N (Rousk & Michelsen, 2017), we do not think that this can explain the excess of N under living trees, especially because mosses as important N fixing species (Zackrisson et al., 2009) are more abundant in the treeless tundra (Figure S1). Notably, birch trees form symbioses with ectomycorrhizal (ECM) fungi that can extend their hyphae several meters (Simard & Durall, 2004) while "mining" the soil for N by decomposing SOM. Friggens et al. (2020) also highlight ectomycorrhizal networks of birch trees that exploit resources throughout a forest. In this context, ECM fungi were reported to stimulate organic matter decomposition (Clemmensen et al., 2021) and hence, to be critically involved in

priming (Paterson et al., 2016; Read & Perez-Moreno, 2003). As a result, litterfall concentrates N that has been acquired from a larger volume of soil, to a smaller area around it. Hence, elevated N stocks below the tree may indeed be indicative of N mining, a process which has also been observed in other mountain birch forests in Fennoscandia (Clemmensen et al., 2021). Yet, locations of excess N stocks do not necessarily match locations where N was mined and the associated priming took place. We suggest that N mining and priming are not exclusively coupled in a spatial way and hypothesize that elevated N stocks, in parts, could originate from SOM decomposition further away from the tree.

We found further indications that priming-induced SOC losses can be considerable, even if this was on average not the case in our study area. Our results revealed considerable variations in SOC stocks and dynamics between the three investigated sites (Figure S3). The finding that site 3 had low SOC stocks under living trees was remarkable, as tree biomass and thus C input to soil was largest compared with the other sites. Also, respiration rates under living trees were at a similar or even higher level at site 3 compared with the other sites (Figure S10), even though site 3 was characterized by lower SOC stocks, similar potential SOC decomposability, and colder temperatures. Hence, root respiration may have a higher contribution to soil +understory respiration at site 3 than in other sites. The amount of root respiration is correlated with the amount of root exudation (Sun et al., 2017), which is one of the main C sources that cause priming (Shahzad et al., 2015). Hence, it can be speculated that larger priming effects are responsible for the low SOC stocks under living trees at site 3. Thus, we suggest that in some cases the high amount of N required by large trees can stimulate SOM decomposition to such an extent that it compensates for elevated SOC inputs (cf. Hartley et al., 2012), making it necessary to conduct these studies on several independent sites simultaneously.

Furthermore, differences in understory vegetation may obscure the relevance of priming-induced SOC losses under living trees. The species composition of understory vegetation differed significantly between living trees and treeless tundra, likely as a result of differences in nutrient supply. Living trees were associated with larger proportions of dwarf shrubs, while treeless tundra was associated with moss and lichen. Also Ylänne et al. (2021) reported a significantly higher proportion of *Vaccinium* sequence reads and higher soil OM content in samples collected from vicinity of mountain birches than samples collected further away from the trees. We could confirm their observation based on the vegetation mapping in our study. It has been reported that C input by the understory vegetation can make a substantial contribution to total soil C input in forests, especially in the north. For instance, Liski et al. (2006) estimated that understory vegetation accounts for an average of 28% of C input across a range of different forest types in Finland. The importance of the understory vegetation may be even greater when exclusively focusing on subarctic birch forests, for example, 35% according to Ding et al. (2019). Hence, the dwarf shrub-dominated understory vegetation may contribute to the observed accumulation of SOC under living trees, especially in the organic layer where 80% of understory root biomass is located (Ding et al., 2019). The finding of greater understory root biomass under living trees in comparison with treeless tundra supports this assumption (Figure 4). Hence, the understory vegetation may obscure the direct effect of trees on SOC stocks, that is, the magnitude of accelerated SOC turnover by birch trees may be underestimated.

Overall, living trees increased the heterogeneity of SOM stocks and dynamics in comparison with treeless tundra. The PCA plot indicates that the treeless tundra clusters in a narrower range in the multidimensional space compared to living trees. This was especially true for mineral soil, where treeless tundra revealed little variation. We assume that differences in tree properties (e.g., age, size, root system, etc.) induce a different degree of priming, N mineralization, and SOC accumulation. This has also been shown by Friggens et al. (2020), suggesting large variations in respiration and mycorrhizosphere productivity between studied trees. Thus, we conclude that trees generate soil heterogeneity, ultimately increasing patchiness of subarctic landscapes.

4.2 | Effect of dead trees on ecosystem carbon stocks and soil organic matter turnover

We originally hypothesized that tree death causes the soil C stocks under the tree to develop toward the C stocks of the treeless tundra, that is, to be in transition between living trees and treeless tundra. Contrary to our expectations, we did not find a consistent development back to tundra-like SOC stocks within 55 years after tree death, that is, SOC stocks under dead trees did not significantly differ from those under living trees. In a short-term study, Sandén et al. (2020) also found no change in SOC stocks within 8 years after tree death. Similarly, no change in SOC stocks was found within 4 years after tree death in boreal *Picea abies* stands caused by a bark beetle outbreak (Kosunen et al., 2020). A continual supply of decaying wood seems to maintain SOC stocks at comparatively high levels, even decades after tree dieback.

In addition to continual supply of decaying wood, elevated SOC stocks under dead trees in comparison with treeless tundra may be further explained by the understory vegetation. Karlsen et al. (2013) and Sandén et al. (2020) reported that moth outbreaks affect the understory vegetation toward a grass-dominated community with consequently labile litter input to soils. We could not confirm this observation in our study, possibly because the appearance of grasses is a short-lived effect caused by the sudden nutrient supply during and shortly after an outbreak event (Vuojala-Magga & Turunen, 2015). Here, the understory community remained unaffected by tree death and resembled that of living trees. Thus, the amount of soil C inputs from understory litter and roots may be similar under living and dead trees, but clearly different from treeless tundra. This can be of quantitative relevance: according to Liski et al. (2006), the understory vegetation was estimated to account for 26% of the total soil C inputs in Finnish forests. This contribution may be even higher in

northern birch forests, that is, 35% according to Ding et al. (2019). Moreover, the composition of SOM may be dominated by recalcitrant litter input from *Empetrum nigrum* (Tybirk et al., 2000), both under living and dead trees, eventually resulting in accumulation of SOM. The combination of ongoing deadwood supply and unaltered C input from understory vegetation may partly explain the unaltered SOC stocks upon tree death.

A further explanation for the unchanged SOC stocks may be a slowed SOM decomposition, which can be assumed for several reasons. First, quality of SOM may change toward a larger proportion of recalcitrant compounds once the most labile compounds of decaying wood have been mineralized (Mackensen & Bauhus, 2003). This, however, was not observed here. Instead, the SOC-normalized respiration did not decrease upon tree death, which indicates similar potential decomposability of SOC under living and dead trees (Fang & Moncrieff, 2005; Mikan et al., 2002). This finding may be partly explained by the unchanged understory vegetation (see above), thereby attenuating the effect of tree death on overall SOC decomposability. Second, the need of vegetation and microorganisms for N may decrease in the absence of trees, tree exudates (Bengtson et al., 2012), and mycorrhiza (Paterson et al., 2016; Read & Perez-Moreno, 2003). Together with the excess of available N in the soil both before (i.e., living trees, Figure 5) and immediately after the moth outbreak event (Kaukonen et al., 2013), N deficiency was likely alleviated after tree death, which may restrict SOM decomposition for the N acquisition, that is, N mining. Indeed, we found lower NO_3 contents and SIR_{cum} under dead trees compared with living trees, which points to smaller amounts of available nutrients. This indicates that SOM turnover—but not potential decomposability of SOM—decreased upon tree death. Lower soil +understory respiration and MBC under dead trees compared with living trees further support this assumption. In summary, the combination of ongoing deadwood supply, unaltered C input from understory vegetation, and slowed SOM turnover may explain why SOC mineralization could not exceed SOC input for at least 55 years after tree death.

Our results of lower N availability, MBC, and soil respiration under dead trees oppose previous observations that mainly covered the short-term effects of moth outbreaks. Such studies mainly referred to the deposition of insect frass, which was reported to be more easily available to microbes than senesced litter (Kristensen et al., 2018), thereby enhancing SOM turnover (Kaukonen et al., 2013). Increases in available N and dissolved organic carbon were also reported, with stimulating effects on MBC and ultimately soil respiration (Kaukonen et al., 2013; Kristensen et al., 2018; Sandén et al., 2020). Here, we did not observe any of these short-term effects that have been observed after moth outbreaks, neither after 12 nor 55 years since the outbreak. This contradiction to previous studies is likely a result of the different time scale considered. Kristensen et al. (2018) speculated that moth outbreaks cause a short-term increase, but long-term decrease in decomposition rates of SOM. Hence, the stimulation of microbial activity upon tree death is likely a short-lived effect triggered by a sudden C and N supply that is not reflected in our data.

Although we found indications for decreasing SOM turnover under dead trees, it did not reach the level of treeless tundra, even after 55 years. Enzyme activities reflect unaltered C or N acquisition strategies of soil microbes upon tree death. Indeed, leaching of dissolved organic carbon from deadwood has been reported, thereby stimulating MBC and respiration (Bantle et al., 2014; Peršoh & Borken, 2017). This effect may persist in the long term. For instance, Minnich et al. (2020) observed elevated MBC and SOC mineralization rates in soil beneath deadwood even 8 years after experimentally placing logs on the forest floor. Furthermore, several studies showed that fungi transfer N from soil to the decaying wood (Oleveira Longa et al., 2018; Philpott et al., 2014; Rinne et al., 2017), hence N mining may continue upon tree death. Such processes may likely be more prominent in our long-term study with more deadwood laying on the forest floor compared to studies that focused on short-term effects of moth outbreaks with standing trees. Hence, N mining and associated priming may continue for a long time after tree death, although at lower rates, and mainly triggered by deadwood instead of root exudates as a source of labile C. This transitional state of dead trees is also visualized by the PCA. In the organic layer, living trees clustered in the lower part of the plot, while treeless tundra was on the upper part and dead trees were in between (Figure 7a). Hence, tree death is accompanied by a transition from a rather N-rich soil with high microbial activity to a N-poor soil with low microbial activity. These changes in soil properties upon tree death indicate a shift in characteristics of biogeochemical cycling toward a state comparable with treeless tundra. Yet, even after 55 years, SOM turnover was still elevated in comparison to treeless tundra.

While SOC stocks remained at an elevated level even decades after moth outbreaks, it should be highlighted that the overall ecosystem carbon stock was clearly reduced by tree death, mainly caused by a decline in aboveground biomass. In such heavily grazed areas, reindeer grazing is a crucial factor in regulating birch growth (Stark et al., 2021), thereby possibly also determining whether birch trees recover or die after moth defoliation (Lehtonen & Heikkinen, 1995). It may also restrict growth of new trees (Biuw et al., 2014; Olofsson et al., 2009). There is clear evidence from published studies that regeneration of birch forest is hampered on the year-round grazed areas on the Finnish side, compared to Norway, where the reindeer migrate seasonally between summer and winter range (Biuw et al., 2014; Kumpula et al., 2011). While the long-term trends in reindeer population densities are quite similar in both countries, the overall reindeer densities in Norway (1.56 reindeer/km² in 2006/2007) are slightly lower than in our study area (2.38 reindeer/km² in 2006/2007; Biuw et al., 2014). Moreover, seasonal migration of reindeer is still practiced in the neighbored areas in Norway, that is, there are separate seasonal pastures with summer grazing in coastal areas, and only winter grazing (i.e., no grazing on birches) in the interior birch forests. In our study area, in contrast, the area is a year-round pasture for reindeer (Biuw et al., 2014). However, it remains uncertain to what extent the lack of forest recovery on our sites was affected by reindeer densities and on the other hand by

historical developments in the study area, preventing the reindeer from going into separate summer and winter pastures. In the circumpolar Arctic, it is more common for the reindeer to migrate seasonally between winter and summer ranges (Stark et al., 2021), which affects the generalization of our findings over a larger geographic scale. In summary, we conclude that in this area, the increased occurrence of moth damage would have minor effects on SOC stocks, but would decrease ecosystem C stocks if the mountain birch forests will not be able to recover from the outbreaks. However, we cannot exclude the possibility that the effect of moth outbreaks on ecosystem C stocks are different in regions that are less heavily affected by grazing, which calls for a comparison of areas with different grazing intensities.

5 | CONCLUSIONS

Our results indicate that trees strengthen the subarctic carbon sink in the Pulmankijärvi area of Finnish Lapland by increasing aboveground and belowground carbon stocks. Forest dieback by severe moth damage may become more frequent in the future due to global warming, and may decrease the total ecosystem C stocks. However, although aboveground biomass decreased upon tree death, SOC stocks under dead trees remained at comparable levels to living trees for at least 55 years. We conclude that the CO_2-related positive feedback of forest disturbance on climate change might be small and very slow in the subarctic region, although only with respect to soil, but not to aboveground stocks. Importantly, our data also highlight considerable spatial variability in the effect of tree status on SOC stocks. This clearly warns against comparing separate sites of living forests, dead forests, and treeless tundra when making predictions about the effect of treeline advancement or recession. We consider the small-scale approach as a more reasonable space-for-time substitution in such patchy landscapes. While our study represents a comprehensive survey of the net effects of mountain birch tree deaths on ecosystem soil C stocks in the Pulmankijärvi area, similar small-scale studies are required in other regions of Fennoscandia to study how generalizable our findings are.

ACKNOWLEDGMENTS

This research was supported by the Academy of Finland (grant number 316401, supporting the salary of K.K.) and Helsinki Institute of Life Science, HiLIFE (a HiLIFE Fellow Grant to K.K supporting, for example, the salary of N.M, and analytical costs). We would like to thank the staff at Kevo Subarctic Research Station for providing research facilities and M. Wallner, L. Menzel, S.-J. Chan, and K. Söllner for help with laboratory work. The authors have no conflict of interest to declare. Open access funding enabled and organized by ProjektDEAL.

DATA AVAILABILITY STATEMENT

The data that support the findings of this study are openly available in Dryad at https://doi.org/10.5061/dryad.p5hqbzkqg.

ORCID

Nele Meyer https://orcid.org/0000-0002-1378-4786
Sylwia Adamczyk https://orcid.org/0000-0002-9051-9302
Christina Biasi https://orcid.org/0000-0002-7413-3354
Lona van Delden https://orcid.org/0000-0003-4332-3160
Angela Martin https://orcid.org/0000-0001-9581-3933
Kevin Mganga https://orcid.org/0000-0002-7908-7561
Kristiina Myller https://orcid.org/0000-0001-6989-0150
Outi-Maaria Sietiö https://orcid.org/0000-0003-0127-9368
Otso Suominen https://orcid.org/0000-0002-7209-6078
Kristiina Karhu https://orcid.org/0000-0003-3101-4141

REFERENCES

Adamczyk, B., Sietiö, O.-M., Straková, P., Prommer, J., Wild, B., Hagner, M., Pihlatie, M., Fritze, H., Richter, A., & Heinonsalo, J. (2019). Plant roots increase both decomposition and stable organic matter formation in boreal forest soil. *Nature Communications*, *10*, 3982. https://doi.org/10.1038/s41467-019-11993-1

Anderson, J. P. E., & Domsch, K. H. (1978). A physiological method for quantitative measurement of microbial biomass in soils. *Soil Biology and Biochemistry*, *10*, 215–221. https://doi.org/10.1016/0038-0717(78)90099-8

Bantle, A., Borken, W., Ellerbrock, R. H., Schulze, E. D., Weisser, W. W., & Matzner, E. (2014). Quantity and quality of dissolved organic carbon released from coarse woody debris of different tree species in the early phase of decomposition. *Forest Ecology and Management*, *329*, 287–294. https://doi.org/10.1016/j.foreco.2014.06.035

Bell, C. W., Fricks, B. E., Rocca, J. D., Steinweg, J. M., McMahon, S. K., & Wallenstein, M. D. (2013). High-throughput fluorometric measurement of potential soil extracellular enzyme activities. *Journal of Visualized Experiments*, *81*, e50961. https://doi.org/10.3791/50961

Bengtson, P., Barker, J., & Grayston, S. J. (2012). Evidence of a strong coupling between root exudation, C and N availability, and stimulated SOM decomposition caused by rhizosphere priming effects. *Ecology and Evolution*, *2*(8), 1843–1852. https://doi.org/10.1002/ece3.311

Biuw, M., Jepsen, J. U., Cohen, J., Ahonen, S. H., Tejesvi, M., Aikio, S., Wäli, P. R., Vindstad, U. P. L., Markkola, A., Niemelä, P., & Ims, R. A. (2014). Long-term impacts of contrasting management of large ungulates in the arctic tundra-forest ecotone: Ecosystem structure and climate feedback. *Ecosystems*, *17*, 890–905. https://doi.org/10.1007/s10021-014-9767-3

Blagodatsky, S., Heinemeyer, O., & Richter, J. (2000). Estimating the active and total soil microbial biomass by kinetic respiration analysis. *Biology and Fertility of Soils*, *32*, 73–81. https://doi.org/10.1007/s003740000219

Carter, M. R., & Gregorich, E. G. (2008). *Soil sampling and methods of analysis* (2nd ed.). Taylor & Francis Group, CRC Press.

Chen, R., Senbayram, M., Blagodatsky, S., Myachina, O., Dittert, K., Lin, X., Blagodatskaya, E., & Kuzyakov, Y. (2014). Soil C and N availability determine the priming effect: Microbial N mining and stoichiometric decomposition theories. *Global Change Biology*, *20*, 2356–2367. https://doi.org/10.1111/gcb.12475

Christensen, T. R., Johansson, T., Olsrud, M., Ström, L., Lindroth, A., Mastepanov, M., Malmer, N., Friborg, T., Crill, P., & Callaghan, T. V. (2007). A catchment-scale carbon and greenhouse gas budget of a subarctic landscape. *Philosophical Transactions of the Royal Society A*, *365*(1856), 1643–1656. https://doi.org/10.1098/rsta.2007.2035

Craine, J. M., Morrow, C., & Fierer, N. (2007). Microbial nitrogen limitation increases decomposition. *Ecology*, *88*, 2105–2113. https://doi.org/10.1890/06-1847.1

Clemmensen, K. E., Durling, M. B., Michelsen, A., Hallin, S., Finlay, R. D., & Lindahl, B. D. (2021). A tipping point in carbon storage when forest expands into tundra is related to mycorrhizal recycling of nitrogen. *Ecology Letters*, *24*, 1193–1204. https://doi.org/10.1890/06-1847.1

Dahl, M. B., Priemé, A., Brejnrod, A., Brusvang, P., Lund, M., Nymand, J., Kramshøj, M., Ro-Poulsen, H., & Haugwitz, M. S. (2017). Warming, shading and a moth outbreak reduce tundra carbon sink strength dramatically by changing plant cover and soil microbial activity. *Scientific Reports*, *7*, 16035. https://doi.org/10.1038/s41598-017-16007-y

Dijkstra, F. A., Bader, N. E., Johnson, D. W., & Cheng, W. (2009). Does accelerated soil organic matter decomposition in the presence of plants increase plant N availability? *Soil Biology and Biochemistry*, *41*(6), 1080–1087. https://doi.org/10.1016/j.soilbio.2009.02.013

Ding, Y., Leppälammi-Kujansuu, J., & Helmisaari, H.-S. (2019). Fine root longevity and below- and aboveground litter production in a boreal Betula pendula forest. *Forest Ecology and Management*, *431*, 17–25. https://doi.org/10.1016/j.foreco.2018.02.039

Fang, C., & Moncrieff, J. B. (2005). The variation of soil microbial respiration with depth in relation to soil carbon composition. *Plant and Soil*, *268*, 243–253. https://doi.org/10.1007/s11104-004-0278-4

Fenner, M. (1997). Evaluation of methods for estimating vegetation cover in a simulated grassland sward. *Journal of Biological Education*, *31*, 49–54. https://doi.org/10.1080/00219266.1997.9655532

Finnish Meteorological Institute. (2020). *Temperature and precipitation statistics from 1961 onwards*. Retrieved from https://en.ilmatietee nlaitos.fi/statistics-from-1961-onwards

Fontaine, S., Bardoux, G., Abbadie, L., & Mariotti, A. (2004). Carbon input to soil may decrease soil carbon content. *Ecology Letters*, *7*, 314–320. https://doi.org/10.1111/j.1461-0248.2004.00579.x

Fontaine, S., Henault, C., Aamor, A., Bdioui, N., Bloor, J. M. G., Maire, V., Mary, B., Revaillot, S., & Maron, P. A. (2011). Fungi mediate long term sequestration of carbon and nitrogen in soil through their priming effect. *Soil Biology and Biochemistry*, *43*(1), 86–96. https://doi.org/10.1016/j.soilbio.2010.09.017

Friggens, N. L., Aspray, T. J., Parker, T. C., Subke, J.-A., & Wookey, P. A. (2020). Spatial patterns in soil organic matter dynamics are shaped by mycorrhizosphere interactions in a treeline forest. *Plant and Soil*, *447*, 521–535. https://doi.org/10.1007/s11104-019-04398-y

Friggens, N. L., Hester, A. J., Mitchell, R. J., Parker, T. C., Subke, J.-A., & Wookey, P. A. (2020). Tree planting in organic soils does not result in net carbon sequestration on decadal timescales. *Global Change Biology*, *26*, 5178–5188. https://doi.org/10.1111/gcb.15229

Hagen, S. B., Jepsen, J. U., Ims, R. A., & Yoccoz, N. G. (2007). Shifting altitudinal distribution of outbreak zones of winter moth Operophtera brumata in sub-arctic birch forest: a response to recent climate warming? *Ecography*, *30*, 299–307. https://doi.org/10.1111/j.0906-7590.2007.04981.x

Hartley, I., Garnett, M., Sommerkorn, M., Hopkins, D. W., Fletcher, B. J., Sloan, V. L., Phoenix, G. K., & Wookey, P. A. (2012). A potential loss of carbon associated with greater plant growth in the European Arctic. *Nature Climate Change*, *2*, 875–879. https://doi.org/10.1038/nclimate1575

Hartley, I. P., Hopkins, D. W., Sommerkorn, M., & Wookey, P. A. (2010). The response of organic matter mineralisation to nutrient and substrate additions in sub-arctic soils. *Soil Biology and Biochemistry*, *42*(1), 92–100. https://doi.org/10.1016/j.soilbio.2009.10.004

Heliasz, M., Johansson, T., Lindroth, A., Mölder, M., Mastepanov, M., Friborg, T., Callaghan, T. V., & Christensen, T. R. (2011). Quantification of C uptake in subarctic birch forest after setback by an extreme insect outbreak. *Geophysical Research Letters*, *38*(1), https://doi.org/10.1029/2010GL044733

Heräjärvi, H. (2004). Variation of basic density and brinell hardness within mature finnish Betula pendula and *B-pubescens* stems. Variation of basic density and Brinell hardness within mature Finnish Betula pendula and *B. pubescens* stems. *Wood and Fiber Science*, *36*, 216–227.

Hicks, L. C., Leizeaga, A., Rousk, K., Michelsen, A., & Rousk, J. (2020). Simulated rhizosphere deposits induce microbial N-mining that may accelerate shrubification in the subarctic. *Ecology*, *101*(9), 3094. https://doi.org/10.1002/ecy.3094

Hinneri, S., Sonesson, M., & Veum, A. K. (1975). Soils of Fennoscandian IBP tundra ecosystems. In F. E. Wielgolaski (Ed.), *Fennoscandian tundra ecosystems*. Ecological Studies (Analysis and Synthesis) (Vol. 16). Springer. https://doi.org/10.1007/978-3-642-80937-8_2

Hofgaard, A., Tømmervik, H., Rees, G., & Hanssen, F. (2012). Latitudinal forest advance in northernmost Norway since the early 20th century. *Journal of Biogeography*, *40*(5), 938–949. https://doi.org/10.1111/jbi.12053

Huttunen, L., Niemelä, P., Ossipov, V., Rousi, M., & Klemola, T. (2012). Do warmer growing seasons ameliorate the recovery of mountain birches after winter moth outbreak? *Trees*, *26*, 809–819. https://doi.org/10.1007/s00468-011-0652-9

ISO 17155. 2012. Soil quality — Determination of abundance and activity of soil microflora using respiration curves. ISO Secretariat, Geneva.

Jepsen, J., Hagen, S., Høgda, K., Ims, R., Karlsen, S., Tømmervik, H., & Yoccoz, N. (2009). Monitoring the spatio-temporal dynamics of geometrid moth outbreaks in birch forest using MODIS-NDVI data. *Remote Sensing of Environment*, *113*, 1939–1947. https://doi.org/10.1016/j.rse.2009.05.006

Jepsen, J. U., Hagen, S. B., Ims, R. A., & Yoccoz, N. G. (2007). Climate change and outbreaks of the geometrids Operophtera brumata and Epirrita autumnata in subarctic birch forest: evidence of a recent outbreak range expansion. *Journal of Animal Ecology*, *77*(2), 257–264. https://doi.org/10.1111/j.1365-2656.2007.01339.x

Karhu, K., Hilasvuori, E., Fritze, H., Biasi, C., Nykänen, H., Liski, J., Vanhala, P., Heinonsalo, J., & Pumpanen, J. (2016). Priming effect increases with depth in a boreal forest soil. *Soil Biology and Biochemistry*, *99*, 104–107. https://doi.org/10.1016/j.soilbio.2016.05.001

Karlsen, S. R., Jepsen, J. U., Odland, A., Ims, R. A., & Elvebakk, A. (2013). Outbreaks by canopy-feeding geometrid moth cause state-dependent shifts in understorey plant communities. *Oecologia*, *173*, 859–870. https://doi.org/10.1007/s00442-013-2648-1

Kaukonen, M., Ruotsalainen, A. L., Wäli, P. R., Männistö, M. K., Setälä, H., Saravesi, K., Huusko, K., & Markkola, A. (2013). Moth herbivory enhances resource turnover in subarctic mountain birch forests? *Ecology*, *94*, 267–272. https://doi.org/10.1890/12-0917.1

Kortesalmi, J. J. (2008). Poronhoidon synty ja kehitys Suomessa. Suomalaisen Kirjallisuuden Seuran toimituksia, SKS, 1149 pp.

Köster, K., Metslaid, M., Engelhart, J., & Köster, E. (2015). Dead wood basic density, and the concentration of carbon and nitrogen for main tree species in managed hemiboreal forests. *Forest Ecology and Management*, *354*, 35–42. https://doi.org/10.1016/j.foreco.2015.06.039

Kosunen, K., Peltoniemi, K., Pennanen, T., Lyytikäinen-Saarenmaa, P., Adamczyk, B., Fritze, H., Zhou, X., & Starr, M. (2020). Storm and Ips typographus disturbance effects on carbon stocks, humus layer carbon fractions and microbial community composition in boreal Picea abies stands. *Soil Biology and Biochemistry*, *148*, 107853. https://doi.org/10.1016/j.soilbio.2020.107853

Krankina, O. N., & Harmon, M. E. (1995). Dynamics of the dead wood carbon pool in northwestern Russian boreal forests. *Water, Air, and Soil Pollution*, *82*, 227–238. https://doi.org/10.1007/BF011 82836

Kristensen, J. A., Metcalfe, D. B., & Rousk, J. (2018). The biogeochemical consequences of litter transformation by insect herbivory in the Subarctic: A microcosm simulation experiment. *Biogeochemistry*, *138*, 323–336. https://doi.org/10.1007/s10533-018-0448-8

Kumpula, J., Stark, S., & Holand, Ø. (2011). Seasonal grazing effects by semi-domesticated reindeer on subarctic mountain birch forests.

Polar Biology, *34*(3), 441–453. https://doi.org/10.1007/s00300-010-0899-4

Kuzyakov, Y., Friedel, J. K., & Stahr, K. (2000). Review of mechanisms and quantification of priming effects. *Soil Biology and Biochemistry*, *32*(11–12), 1485–1498. https://doi.org/10.1016/S0038-0717(00)00084-5

Lehmann, J., & Kleber, M. (2015). The contentious nature of soil organic matter. *Nature*, *528*, 60–68. https://doi.org/10.1016/S0038-0717(00)00084-5

Lehtonen, J., & Heikkinen, R. K. (1995). On the recovery of mountain birch after Epirrita damage in Finnish Lapland, with a particular emphasis on reindeer grazing. *Écoscience*, *2*(4), 349–356. https://doi.org/10.1080/11956860.1995.11682303

Liski, J., Lehtonen, A., Palosuo, T., Peltoniemi, M., Eggers, T., Muukkonen, P., & Mäkipää, R. (2006). Carbon accumulation in Finland's forests 1922–2004 – An estimate obtained by combination of forest inventory data with modelling of biomass, litter and soil. *Annals of Forest Science*, *63*(7), 687–697. https://doi.org/10.1051/forest:2006049

Mackensen, J., & Bauhus, J. (2003). Density loss and respiration rates in coarse woody debris of Pinus radiata, Eucalyptus regnans and Eucalyptus maculata. *Soil Biology and Biochemistry*, *35*, 177–186. https://doi.org/10.1016/S0038-0717(02)00255-9

Marx, M. C., Wood, M., & Jarvis, S. C. (2001). A microplate fluorimetric assay for the study of enzyme diversity in soils. *Soil Biology and Biochemistry*, *33*, 1633–1640. https://doi.org/10.1016/S0038-0717(01)00079-7

Meyer, N., Welp, G., Bornemann, L., & Amelung, W. (2017). Microbial nitrogen mining affects spatio-temporal patterns of substrate-induced respiration during seven years of bare fallow. *Soil Biology and Biochemistry*, *104*, 175–184. https://doi.org/10.1016/j.soilbio.2016.10.019

Meyer, N., Welp, G., Rodionov, A., Borchard, N., Martius, C., & Amelung, W. (2018). Nitrogen and phosphorus supply controls soil organic carbon mineralization in tropical topsoil and subsoil. *Soil Biology and Biochemistry*, *119*, 152–161. https://doi.org/10.1016/j.soilbio.2018.01.024

Meyer, N., Xu, Y., Karjakainen, K., Adamczyk, S., Biasi, C., van Delden, L., Martin, A., Mganga, K., Myller, K., Sietiö, O.-M., Suominen, O., & Karhu, K. (2021). Data from: Living, dead, and absent trees - How do moth outbreaks shape small-scale patterns of soil organic matter stocks and dynamics at the Subarctic mountain birch treeline? Dryad, Dataset, https://doi.org/10.5061/dryad.p5hqbzkqg

Mikan, C. J., Schimel, J. P., & Doyle, A. P. (2002). Temperature controls of microbial respiration in arctic tundra soils above and below freezing. *Soil Biology and Biochemistry*, *34*(11), 1785–1795. https://doi.org/10.1016/S0038-0717(02)00168-2

Mikola, J., Silfver, T., & Rousi, M. (2018). Mountain birch facilitates Scots pine in the northern tree line–does improved soil fertility have a role? *Plant and Soil*, *423*, 205–213. https://doi.org/10.1007/s11104-017-3517-1

Minnich, C., Peršoh, D., Poll, C., & Borken, W. (2020). Changes in chemical and microbial soil parameters following 8 years of deadwood decay: An experiment with logs of 13 tree species in 30 forests. *Ecosystems*, *24*(4), 955–967. https://doi.org/10.1007/s10021-020-00562-z

Miranda, K. M., Espey, M. G., & Wink, D. A. (2001). A rapid, simple spectrophotometric method for simultaneous detection of nitrate and nitrite. *Nitric Oxide*, *5*, 62–71. https://doi.org/10.1006/niox.2000.0319

Moorhead, D. L., & Sinsabaugh, R. L. (2006). A theoretical model of litter decay and microbial interaction. *Ecological Monographs*, *76*, 151–174. https://doi.org/10.1890/0012-9615(2006)076[0151:ATMOLD]2.0.CO;2

Neuvonen, S., Niemelä, P., & Virtanen, T. (1999). Climatic change and insect outbreaks in boreal forests: The role of winter temperatures. *Ecological Bulletins*, *47*, 63–67. https://www.jstor.org/stable/20113228

Nordgren, A. (1988). Apparatus for the continuous long-term monitoring of soil respiration rate in large numbers of samples. *Soil Biology and Biochemistry*, *20*, 955–958. https://doi.org/10.1016/0038-0717(88)90110-1

Nordgren, A. (1992). A method for determining microbially available N and P in an organic soil. *Biology Fertility of Soils*, *13*, 195–199. https://doi.org/10.1007/BF00340575

Nuorteva, P. (1963). The influence of Oporinia autumnata (Bkh.) (Lep., Geometridae) on the timberline in subarctic conditions. *Annales Entomologici Fennici*, *29*, 270–277.

Oliveira Longa, C. M., Francioli, D., Gómez-Brandón, M., Ascher-Jenull, J., Bardelli, T., Pietramellara, G., Egli, M., Sartori, G., & Insam, H. (2018). Culturable fungi associated with wood decay of Picea abies in subalpine forest soils: a field-mesocosm case study. *Forest*, *11*, 781–785. https://doi.org/10.3832/ifor2846-011

Olofsson, J., Oksanen, L., Callaghan, T., Hulme, P. E., Oksanen, T., & Suominen, O. (2009). Herbivores inhibit climate-driven shrub expansion on the tundra. *Global Change Biology*, *15*, 2681–2693. https://doi.org/10.1111/j.1365-2486.2009.01935.x

Olsson, P.-O., Heliasz, M., Jin, H., & Eklundh, L. (2017). Mapping the reduction in gross primary productivity in subarctic birch forests due to insect outbreaks. *Biogeosciences*, *14*, 1703–1719. https://doi.org/10.5194/bg-14-1703-2017

Parker, T. C., Sadowsky, J., Dunleavy, H., Subke, J.-A., Frey, S. D., & Wookey, P. A. (2017). Slowed biogeochemical cycling in Sub-arctic birch forest linked to reduced mycorrhizal growth and community change after a defoliation Event. *Ecosystems*, *20*, 316–330. https://doi.org/10.1007/s10021-016-0026-7

Parker, T. C., Subke, J.-A., & Wookey, P. A. (2015). Rapid carbon turnover beneath shrub and tree vegetation is associated with low soil carbon stocks at a subarctic treeline. *Global Change Biology*, *21*(5), 2070–2081. https://doi.org/10.1111/gcb.12793

Paterson, E., Sim, A., Davidson, J., & Daniell, T. J. (2016). Arbuscular mycorrhizal hyphae promote priming of native soil organic matter mineralisation. *Plant and Soil*, *408*, 243–254. https://doi.org/10.1007/s11104-016-2928-8

Peršoh, D., & Borken, W. (2017). Impact of woody debris of different tree species on the microbial activity and community of an underlying organic horizon. *Soil Biology and Biochemistry*, *115*, 516–525. https://doi.org/10.1016/j.soilbio.2017.09.017

Philpott, T. J., Prescott, C. E., Chapman, W. K., & Grayston, S. J. (2014). Nitrogen translocation and accumulation by a cord-forming fungus (Hypholoma fasciculare) into simulated woody debris. *Forest Ecology and Management*, *315*, 121–128. https://doi.org/10.1016/j.foreco.2013.12.034

R Core Team (2013). *R: A language and environment for statistical computing*. R Foundation for Statistical Computing. http://www.R-project.org/

Rapalee, G., Trumbore, S. E., Davidson, E. A., Harden, J. W., & Veldhuis, H. (1998). Soil carbon stocks and their rates of accumulation and loss in a boreal forest landscape. *Global Biogeochemical Cycles*, *12*(4), 687–701. https://doi.org/10.1029/98GB02336

Read, D. J., & Perez-Moreno, J. (2003). Mycorrhizas and nutrient cycling in ecosystems – A journey towards relevance? *New Phytologist*, *157*(3), 475–492. https://doi.org/10.1046/j.1469-8137.2003. 00704.x

Rinne, K. T., Rajala, T., Peltoniemi, K., Chen, J., Smolander, A., & Mäkipää, R. (2017). Accumulation rates and sources of external nitrogen in decaying wood in a Norway spruce dominated forest. *Functional Ecology*, *31*, 530–541. https://doi.org/10.1111/1365-2435.12734

Rousk, K., & Michelsen, A. (2017). Ecosystem nitrogen fixation throughout the snow-free period in subarctic tundra: Effects of willow and birch litter addition and warming. *Global Change Biology*, *23*(4), 1552–1563. https://doi.org/10.1111/gcb.13418

Rundqvist, S., Hedenås, H., Sandström, A., Emanuelsson, U., Eriksson, H., Jonasson, C., & Callaghan, T. V. (2011). Tree and shrub expansion over the past 34 years at the tree-line near Abisko, Sweden. *Ambio*, *40*(6), 683–692. https://doi.org/10.1007/s13280-011-0174-0

Russell, M. B., Fraver, S., Aakala, T., Gove, J. H., Woodall, C. W., D'Amato, A. W., & Ducey, M. J. (2015). Quantifying carbon stores and decomposition in dead wood: A review. *Forest Ecology and Management*, *350*, 107–128. https://doi.org/10.1016/j.foreco.2015.04.033

Sandén, H., Mayer, M., Stark, S., Sandén, T., Nilsson, L. O., Jepsen, J. U., Wäli, P. R., & Rewald, B. (2020). Moth outbreaks reduce decomposition in Subarctic forest soils. *Ecosystems*, *23*, 151–163. https://doi.org/10.1007/s10021-019-00394-6

Saravesi, K., Aikio, S., Wäli, P. R., Ruotsalainen, A. L., Kaukonen, M., Huusko, K., Suokas, M., Brown, S. P., Jumpponen, A., Tuomi, J., & Markkola, A. (2015). Moth outbreaks alter root-associated fungal communities in Subarctic mountain birch forests. *Microbial Ecology*, *69*, 788–797. https://doi.org/10.1007/s00248-015-0577-8

Schielzeth, H., Dingemanse, N. J., Nakagawa, S., Westneat, D. F., Allegue, H., Teplitsky, C., Réale, D., Dochtermann, N. A., Garamszegi, L. Z., & Araya-Ajoy, Y. G. (2020). Robustness of linear mixed-effects models to violations of distributional assumptions. *Methods in Ecology and Evolution*, *2020*(11), 1141–1152. https://doi.org/10.1111/2041-210X.13434

Schmidt, M., Torn, M., Abiven, S., Dittmar, T., Guggenberger, G., Janssens, I. A., Kleber, M., Kögel-Knabner, I., Lehmann, J., Manning, D. A. C., Nannipieri, P., Rasse, D. P., Weiner, S., & Trumbore, S. E. (2011). Persistence of soil organic matter as an ecosystem property. *Nature*, *478*, 49–56. https://doi.org/10.1038/nature10386

Shahzad, T., Chenu, C., Genet, P., Barot, S., Perveen, N., Mougin, C., & Fontaine, S. (2015). Contribution of exudates, arbuscular mycorrhizal fungi and litter depositions to the rhizosphere priming effect induced by grassland species. *Soil Biology and Biochemistry*, *80*, 146–155. https://doi.org/10.1016/j.soilbio.2014.09.023

Silfver, T., Heiskanen, L., Aurela, M., Myller, K., Karhu, K., Meyer, N., Tuovinen, J.-P., Oksanen, E., Rousi, M., & Mikola, J. (2020). Insect herbivory dampens Subarctic birch forest C sink response to warming. *Nature Communications*, *11*, 2529. https://doi.org/10.1038/s41467-020-16404-4

Simard, S. W., & Durall, D. M. (2004). Mycorrhizal networks: A review of their extent, function, and importance. *Canadian Journal of Botany*, *82*, 1140–1165. https://doi.org/10.1139/b04-116

Sjögersten, S., & Wookey, P. A. (2004). Decomposition of mountain birch leaf litter at the forest-tundra ecotone in the Fennoscandian mountains in relation to climate and soil conditions. *Plant and Soil*, *262*, 215–227. https://doi.org/10.1023/B:PLSO.0000037044.63113.fe

Smith, A., Granhus, A., & Astrup, R. (2016). Functions for estimating belowground and whole tree biomass of birch in Norway. *Scandinavian Journal of Forest Research*, *31*, 568–582. https://doi.org/10.1080/02827581.2016.1141232

Stark, S., Ylänne, H., & Kumpula, J. (2021). Recent mountain birch ecosystem change depends on the seasonal timing of reindeer grazing. *Journal of Applied Ecology*, *58*, 941–952. https://doi.org/10.1111/1365-2664.13847

Starr, M., Hartman, M., & Kinnunen, T. (1998). Biomass functions for mountain birch in the Vuoskojärvi Integrate Monitoring area. *Boreal Environment Research*, *3*, 297–303.

Štursová, M., Šnajdr, J., Cajthaml, T., Bárta, J., Šantrůčková, H., & Baldrian, P. (2014). When the forest dies: the response of forest soil fungi to a bark beetle-induced tree dieback. *The ISME Journal*, *8*, 1920–1931. https://doi.org/10.1038/ismej.2014.37

Sun, L., Ataka, M., Kominami, Y., & Yoshimura, K. (2017). Relationship between fine-root exudation and respiration of two Quercus species in a Japanese temperate forest. *Tree Physiology*, *37*(8), 1011–1020. https://doi.org/10.1093/treephys/tpx026

Tenow, O. (1996). Hazards to a mountain birch forest - Abisko in perspective. *Ecological Bulletins*, *45*, 104–114. https://www.jstor.org/stable/20113188

Tømmervik, H., Johansen, B., Tombre, I., Thannheiser, D., Høgda, K. A., Gaare, E., & Wielgolaski, F. E. (2004). Vegetation changes in the nordic mountain birch forest: the influence of grazing and climate change. *Arctic, Antarctic, and Alpine Research*, *36*(3), 323–332. https://doi.org/10.1657/1523-0430(2004)036[0323:VCITNM]2.0.CO;2

Tybirk, K., Nilsson, M.-C., Michelsen, A., Kristensen, H. L., Shevtsova, A., Strandberg, M. T., Johansson, M., Nielsen, K. E., Riis-Nielsen, T., Strandberg, B., & Johnsen, I. (2000). Nordic Empetrum dominated ecosystems: Function and susceptibility to environmental changes. *Ambio*, *29*, 90–97. https://doi.org/10.1579/0044-7447-29.2.90

Vuojala-Magga, T., & Turunen, M. T. (2015). Sámi reindeer herders' perspective on herbivory of subarctic mountain birch forests by geometrid moths and reindeer: a case study from northernmost Finland. *SpringerPlus*, *4*, 134. https://doi.org/10.1186/s40064-015-0921-y

Wang, H., Xu, W., Hu, G., Dai, W., Jiang, P., & Bai, E. (2015). The priming effect of soluble carbon inputs in organic and mineral soils from a temperate forest. *Oecologia*, *178*, 1239–1250. https://doi.org/10.1007/s00442-015-3290-x

Wilmking, M., Harden, J., & Tape, K. (2006). Effect of tree line advance on carbon storage in NW Alaska. Journal of Geophysical Research. *Biogeosciences*, *111*(G2), https://doi.org/10.1029/2005JG000074

WRB, IUSS Working Group. (2015). World Reference Base for Soil Resources 2014, update 2015 International soil classification system for naming soils and creating legends for soil maps. World Soil Resources Reports No. 106. FAO. Rome.

Ylänne, H., Madsen, R. L., Castaño, C., Metcalfe, D. B., & Clemmensen, K. E. (2021). Reindeer control over subarctic treeline alters soil fungal communities with potential consequences for soil carbon storage. *Global Change Biology*, *27*, 4254–4268. https://doi.org/10.1111/gcb.15722

Zackrisson, O., DeLuca, T. H., Gentili, F., Sellstedt, A., & Jäderlund, A. (2009). Nitrogen fixation in mixed Hylocomium splendens moss communities. *Oecologia*, *160*, 309–319. https://doi.org/10.1007/s00442-009-1299-8

SUPPORTING INFORMATION

Additional supporting information may be found in the online version of the article at the publisher's website.

How to cite this article: Meyer, N., Xu, Y., Karjalainen, K., Adamczyk, S., Biasi, C., van Delden, L., Martin, A., Mganga, K., Myller, K., Sietiö, O.-M., Suominen, O., & Karhu, K. (2022). Living, dead, and absent trees—How do moth outbreaks shape small-scale patterns of soil organic matter stocks and dynamics at the Subarctic mountain birch treeline? *Global Change Biology*, 28, 441–462. https://doi.org/10.1111/gcb.15951